ELECTRICAL STIMULATION OF MUSCLES WITH APPLICATION TO FACIAL PARALYSIS

by

Doreen K. Jacob

BSME, University of Pittsburgh, 2002

Submitted to the Graduate Faculty of

School of Engineering in partial fulfillment

of the requirements for the degree of

Master of Science Mechanical Engineering

University of Pittsburgh

2004

UNIVERSITY OF PITTSBURGH

SCHOOL OF ENGINEERING

This thesis was presented

by

Doreen K. Jacob

It was defended on

April 6, 2004

and approved by

Dr. Roy D. Marangoni, Associate Professor, Dept. of Mechanical Engineering

Dr. Marlin H. Mickle, Professor, Dept. of Electrical Engineering

Thesis Advisor: Dr. Michael R. Lovell, Associate Dean for Research, Dept. of Mechanical Engineering

ELECTRICAL STIMULATION OF MUSCLES WITH APPLICATION TO FACIAL PARALYSIS

Doreen K. Jacob, MSME

University of Pittsburgh, 2004

Facial nerve paralysis is a condition that is typically caused by injury to the seventh cranial facial nerve that controls the muscle movements and expressions of the face. Facial paralysis is often due to Bell's Palsy. The most common cause of this ailment is the herpes simplex virus type 1, which causes inflammation. As the facial nerve (cranial nerve VII) passes through the narrow auditory canal, it inflames, becomes constricted, and prevents transmission of signals from the facial nerve to the muscles of the face. When the facial nerve is compressed, visible defects including sagging of the eyelid, cheek and mouth occurs. The major concern with this type of nerve damage, however, is the loss of dynamic blink of the eyelid. The eyelid serves as a shield from tiny foreign materials. The inability to blink may result in damaging conditions that include dry eyes, infections and visual impairment. There are a number of treatments to help protect the eye; however, no treatments are currently able to restore the eye blink. In order to reanimate the eye, the orbicularis muscle must be stimulated by another means, such as electrical stimulus. Therefore in the present research, different levels of current will be used to stimulate the gastrocnemius leg muscle of Sprague-Dawley rats to determine the optimum range of current that elicits a muscle contraction without causing damage to the tissue. These experiments will be performed using a specialized Mass Immunization Device, which pulses current to simulate an

eye blink and calculates the resistance of the muscle tissue during each pulse. The range of current tested was between 0.005 and 37.3 milliamps. Based on the experimental results, the tissue resistance was found to decrease with higher levels of currents and with each electrical pulse. For the application targeted in this project, current at the micro-amp level is preferred so that tissue damage does not result.

TABLE OF CONTENTS

LIST OF TABLES

LIST OF FIGURES

ACKNOWLEDGEMENTS

First, I would like to thank Dr. Tonya Stefko and the University of Pittsburgh Medical Center for giving me the opportunity to be involved in such a cutting edge project. Working on a project such as this has reinforced my desire to become involved in areas with medically related applications. Next, I would especially like to thank my advisor, Dr. Michael Lovell, for his guidance, patience and encouragement throughout the course of this project. In addition, I extend my appreciation to Dr. Marlin Mickle who has also dedicated his time and effort in directing me during this project. Finally, I would like to thank the students who developed the Mass Immunization Device for their time and creativity.

I dedicate this project to my family and loved ones, their love and support has allowed and encouraged me to take on new challenges and achieve more than I thought possible.

1.0 INTRODUCTION

Facial paralysis due to ailments such as Bell's Palsy, is the result of damage or injury to the facial nerve that controls the muscle movements and the expressions of the face. Although the exact cause of Bell's Palsy is unknown, the result is damage to the seventh cranial nerve (see Figure 1). A number of etiologies can lead to this disease, but the majority is due to a viral infection that causes inflammation. When the inner auditory canal or fallopian canal in which the seventh cranial nerve passes becomes constricted, transmissions of signals by the facial nerves to the muscles of the face are prevented (see Figure 2). The most frequent cause of this inflammation is known to be the herpes simplex virus type 1. Other causes of facial paralysis include tumor, trauma, nerve injury, infection and generalized polyneuritis.

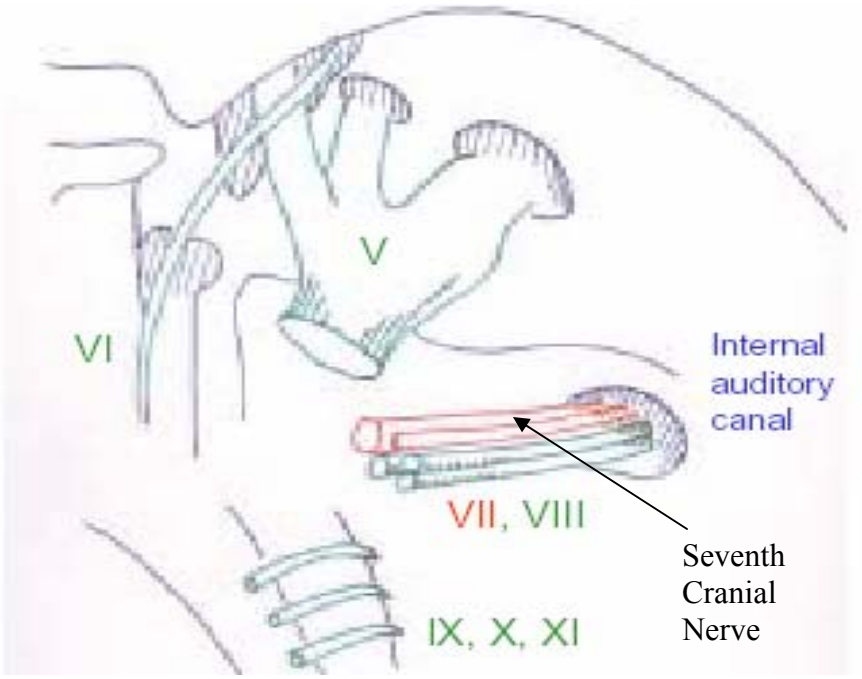

Figure 1. Cranial nerve VII passing through the narrow internal auditory canal [1].

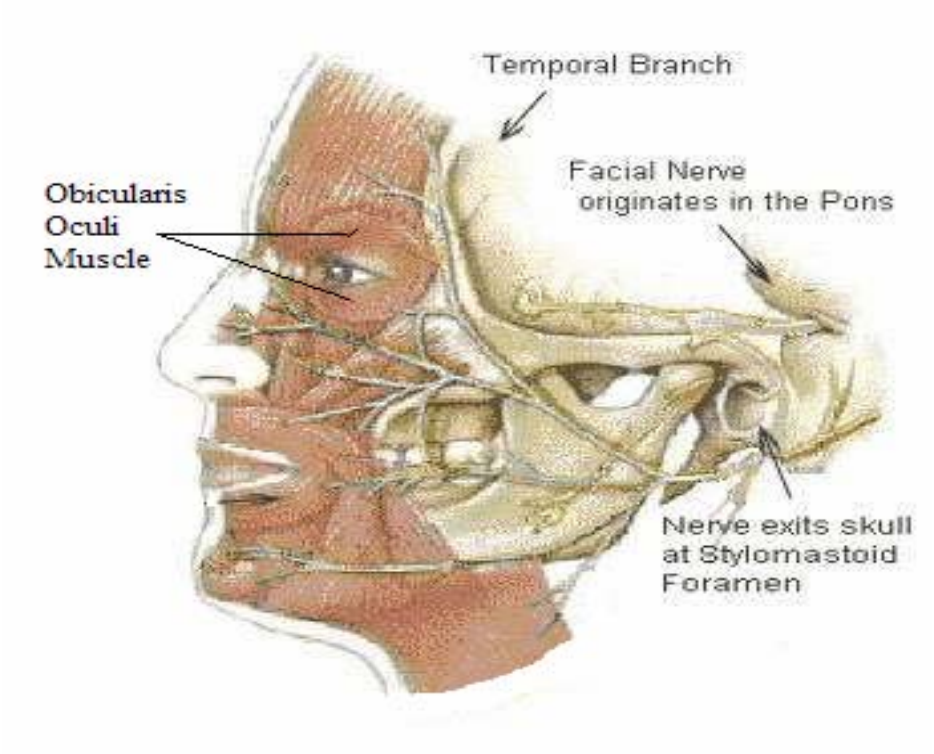

Figure 2. Facial nerve branching out to the face [2].

1.1 LITERATURE SURVEY

Facial nerve damage causes visible defects such as loss of blink and sagging of the cheek and mouth. The major concern with facial paralysis is the loss of dynamic blink of the eyelid. Eyelid closure is essential for corneal protection, given that it serves as a shield from tiny objects and foreign materials from entering the eye. It also lubricates the cornea, preventing dry eyes, and washes away any dirt or other debris that has entered. The inability to blink can result in severe dry eyes, infections, and visual impairment [3].

Although there are many treatments for facial nerve paralysis, most of them only provide temporary protection to the corneal surface and do not restore the loss of blink. Tarsorrhaphy is a common medical procedure that narrows the space between the eyelids in order to cover the eye, by suturing together the margins of the eyelids. This procedure not only reduces peripheral vision and is disfiguring, but it also can cause scarring to the cornea [4]. Unfortunately even after surgery, this procedure requires the use of artificial lubrication for the cornea [5]. The use of gold weights implanted in the upper eyelid is another procedure used to protect the eye. With the help of gravity, the gold weight assists in closing the eyelid when the muscle in the upper lid is relaxed [3]. Implantation of gold weights reduces lagophthalmos, and provides and improves the amplitude of closure during blinking [6]. Its bulk, however, produces visible deformities and does restore reflex eyelid closure [7].

Another alternative to reanimation is to undergo facial surgery. Surgical decompression of the facial nerve can be done to restore and improve motor and sensory functions [8]. This procedure does not benefit patients unless it is performed within 14 days of total paralysis [8]. Cross-face nerve grafting surgery is another measure taken for facial restoration. Although this procedure can improve the voluntary movement of the eye, improvements take 6-12 months and may require more than one surgery [9, 5]. It may also weaken the muscle activity on the normal side, while only minor improvements on the affected side may occur [10]. In general, it has been shown that the time in which facial paralysis occurs and the time that the surgery is performed is crucial and should be done within a year of denervation [11].

Reanimation of the eyelid has been treated by electrical stimulation therapy. This treatment initiates contraction in the paralyzed eyelid. Experiments have shown that electrical stimulation for unilateral facial paralysis improves patients with ongoing facial paralysis by

stimulating the nerve on the paretic side. This stimulation restores facial control and lessens synkineisis [12, 13]. Due to the use of high voltage and current (to overcome skin resistance) skin irritation may occur [14]. Reviewing the literature in this area, Somia et al compared the effects of a single-channel versus a multi-channel electrical stimulation of eyelid mechanics in a dog model [5]. After inserting electrodes into the orbicularis oculi muscle (OOM), a complete eye closure was obtained when certain areas of the OOM were stimulated at low current strengths. A multi-channel set up was found to be preferable since it takes less current to stimulate a contraction and therefore is not painful [5].

Fully implantable stimulators have also been used in the area of functional electric stimulation [15]. There are studies currently underway to develop wireless devices that can be used to treat paralyzed muscles. Experiments have been performed, for example, using implantable stimulators to initiate contraction in denervated muscles. Dennis et al developed an implantable battery powered device to generate contractions in enervated hind-limb muscles of rats to maintain muscle mass and maximum force in stimulated – denervated extensor digitorum longus (EDL) muscles [16]. Similar to this idea are the BIOnic Neuron devices. These are multiple stimulating mechanisms, which are implanted directly into the muscle that generate digitally controlled, current regulated pulses by the use of an external control box and transmission coil that powers and commands the implant functions [14].

1.2 THE FOCUS OF THIS PROJECT

The ultimate goal of this project is to develop a device that will restore blink in patients diagnosed with facial nerve paralysis. This device will consist of tiny silicon chips that will

function as both sensors and actuators. Once the circuitry is constructed, it will be integrated into the chip along with electrodes that are used to stimulate the eye muscles. The silicon chip will be designed with a radio frequency based microelectrode system that will be implanted into the face. The system will coordinate stimulation of one orbicularis muscle to enable contraction in concert with the normal side. A radio frequency power source for the device will be incorporated into a pair of glasses that will be worn on the patients face, near the implanted chips. A flow chart of this process is illustrated in Figure 3. As highlighted in the figure, this thesis will focus on determining the optimal range for muscle stimulation of such a device.

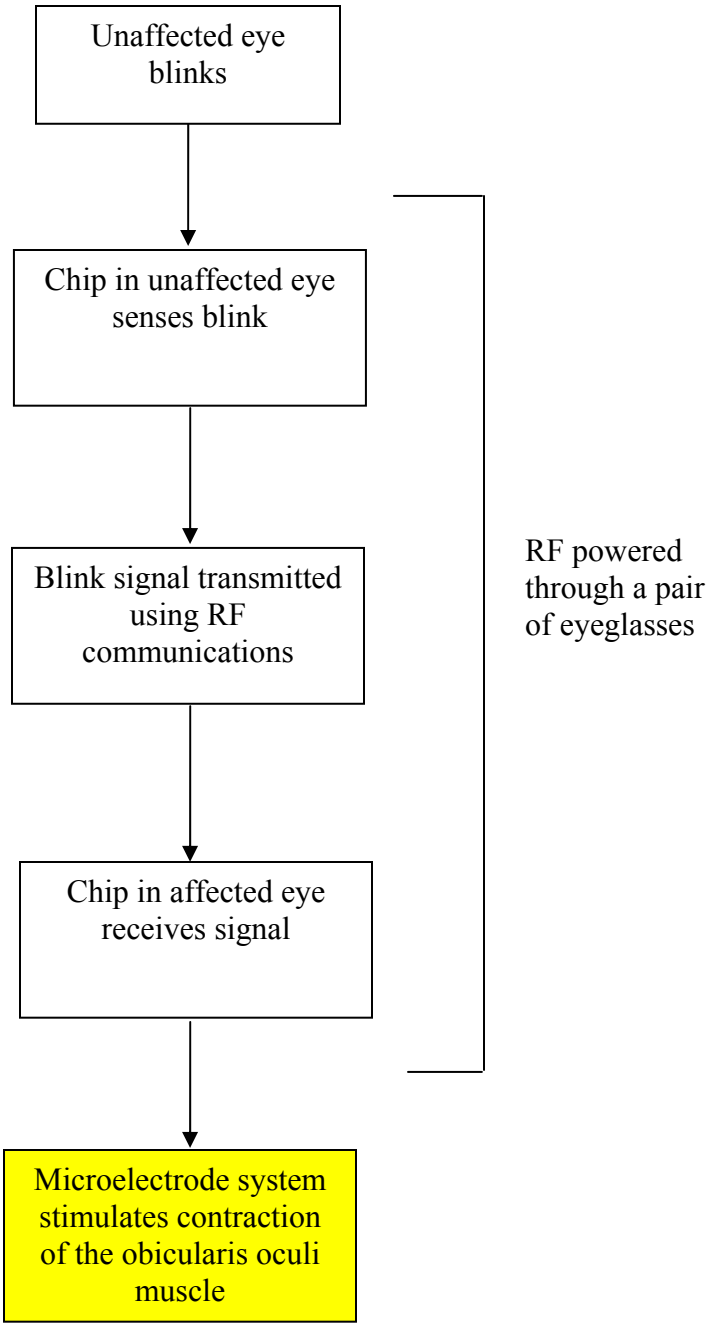

Figure 3. A flow chart for the microelectrode device.

In order to develop the microelectrode system, in vivo testing is required to determine the optimum stimulation for producing a muscle contraction. These tests will initially be performed on the gastrocnemius muscles of rats using a device that enables variation in electrical stimulus and determines muscle resistance. The device will measure the resistance of the muscle tissue with the entered voltage, pulse count and pulse width, and will incorporate a current limiting circuit that will regulate the amount of current stimulating the muscle. After each muscle is stimulated, its response will be measured and later the tissue examined for burned tissue. It will then be categorized as no response, muscle contracted and no tissue burned, muscle contracted and tissue burned, or tissue burned. With this information, the optimal range of current to stimulate muscle contraction without causing tissue damage can be determined and the electrical properties of the silicon chip can be determined. Once the chip is assembled, the placement of the chip in the face must be determined.

2.0 BACKGROUND ON MUSCLE STIMULATION AND CONTRACTION

In order for a muscle to contract, an action potential, or a change in membrane potential must be produced on the membrane of the nerve or muscle fibers. An action potential is a result of mechanical, chemical or electrical disturbance on the membrane. Initially, the inside of the membrane has a potential of -90 millivolts with respect to the outside. This initial state is called the resting state. Surrounding the membrane are positively and negatively charged ions, which permeate the membrane when certain voltage-gated channels on the membrane are open.

When an action potential occurs by electrical stimulation, the potential across the membrane decreases. The negative current from the electrode decreases the voltage on the outside of the membrane to a negative value nearer to the voltage on the inside of the fiber**.** This decrease in membrane potential causes the opening of the sodium channels, allowing positive sodium ions to flow into the membrane, resulting in a more positive potential on the membrane interior. This process is known as the depolarization state.

After the membrane becomes permeable to sodium ions, the sodium channels close and the potassium channels open. The potassium exits the interior of the membrane and restores it to the normal resting membrane potential. This is referred to as repolarization. Figure 4 refers to the flow of ions through the voltage gated sodium and potassium channels.

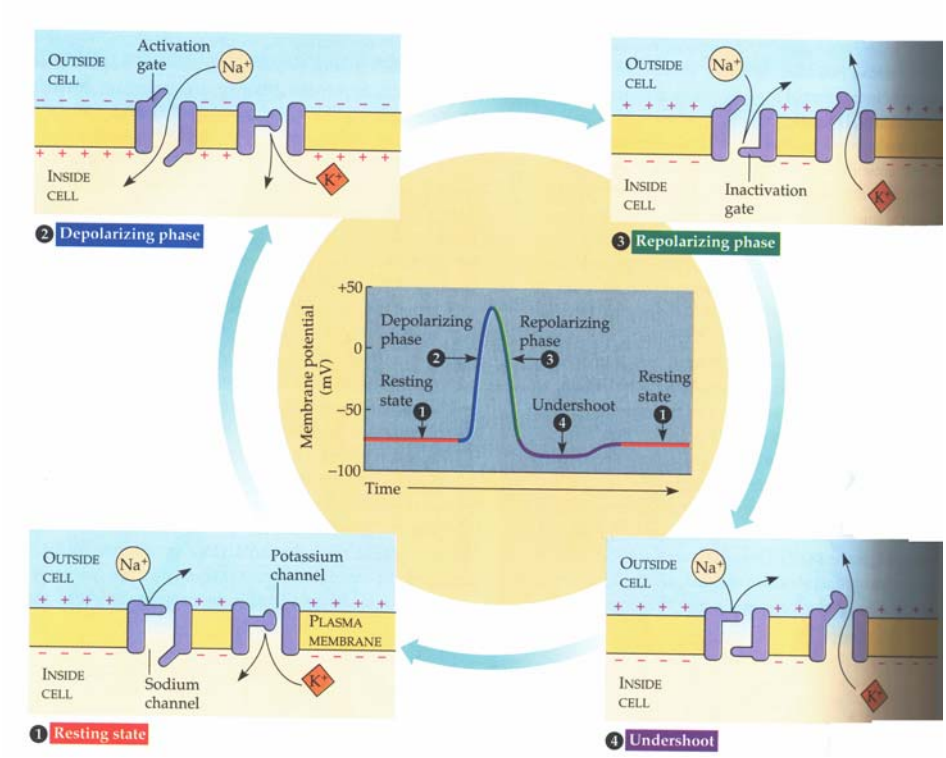

Figure 4. Voltage gated sodium and potassium channels [17].

In skeletal muscles, each muscle fiber is composed of a bundle of several thousand smaller myofibrils. Each myofibril contains two types of myofilaments, myosin and actin. The thick filaments or the myosin filaments are arrays of myosin molecules. The myosin is composed of a long fibrous tail with a round head protruding off to the side. The tail is where the myosin molecules attach to the myosin filaments. The thin filaments consist of two strands of actin and one strand of regulatory protein twisting around one another. The actin molecules contain myosin binding sites. When the muscle is at rest, a regulatory protein called tropomyosin covers the myosin binding receptor sites on actin molecules. Another regulatory protein called the troponin complex, regulates the location of the tropomyosin on the actin filament. A diagram of this is shown in Figures 5 and 6.

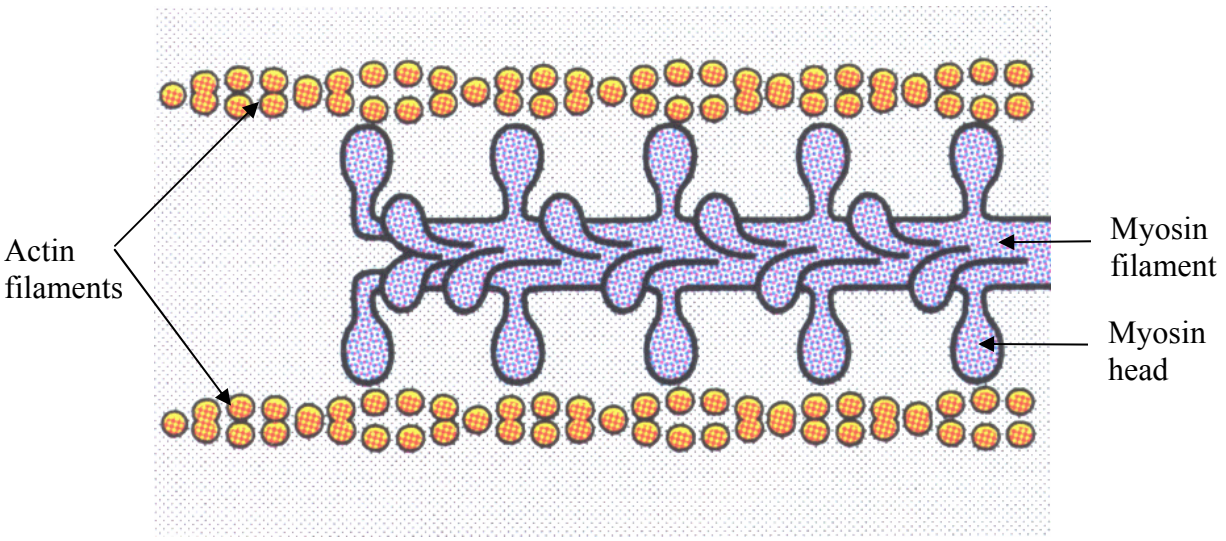

Figure 5. Myosin and actin filaments [18].

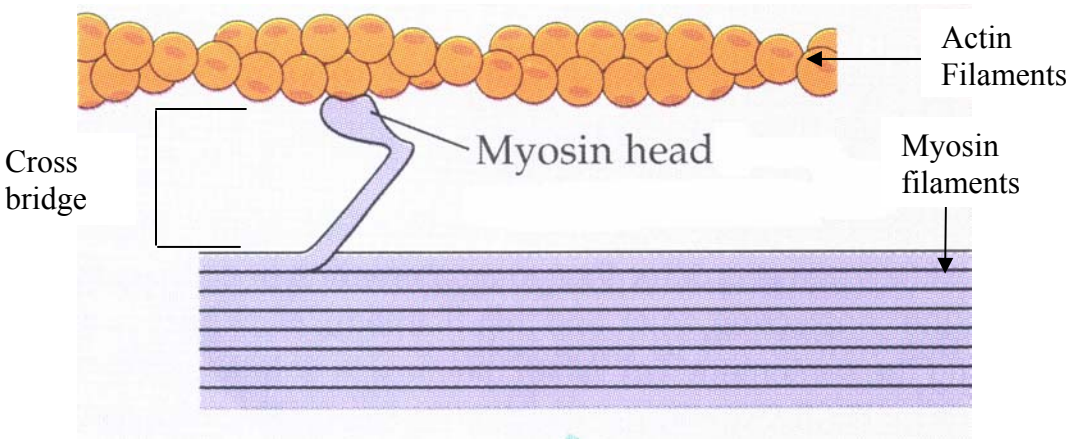

Figure 6. Myosin head forming a cross bridge with actin filament [19].

When an action potential occurs, it travels along a motor nerve to the interface with the muscle fibers. The nerve discharges a neurotransmitter substance called acetylcholine. The acetylcholine triggers multiple acetylcholine-gated channels to open on the muscle fiber membrane, through protein molecules suspended in the membrane. These gated channels permit large amounts of sodium ions to enter into the interior of the muscle fiber membrane to initiate an action potential in the muscle fiber. When the action potential travels along the muscle fiber membranes, it depolarizes the muscle membrane. As the action potential spreads into the interior of the muscle, it travels along folds of the plasma membrane called transverse tubules. These tubules contact the sarcoplasmic reticulum causing it to change its permeability and therefore, causing the sarcoplasmic reticulum to release large amounts of positively charged calcium ions. When the calcium ions are discharged, they bind to the troponin complex, causing the tropomyosin and troponin complex to change shape. This in turn, causes the myosin binding sites to be exposed on the actin and the myosin head binds to a specific site on the actin, forming a cross bridge, pulling the thin filaments toward the sarcomere, which results in a muscle contraction (see Figure 7).

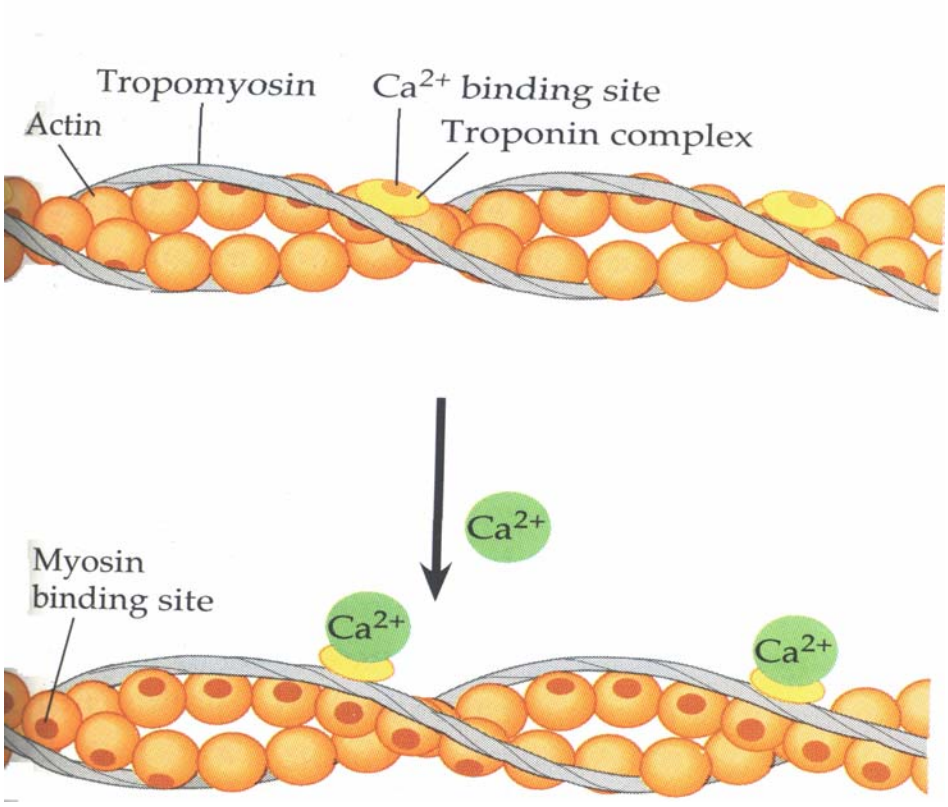

Figure 7. Myosin binding sites are exposed when calcium is released allowing for muscle contraction [20].

The myofilaments create a pattern of light and dark bands in the muscle. Each repeated unit of the light and dark bands is referred to as the sarcomere. It lies between two Z discs, which are attached to the ends of the actin filaments and are projected towards the middle in the sarcomere. The myosin filaments are centered in the sarcomere. At resting length the actin filaments somewhat overlap each other. Other parts of the muscle are I bands, A bands and H zones. The I bands are the light bands that only contain the actin filaments. They are called I bands because they are isotropic to polarized light. The A bands are the dark bands and correspond to the length of the myosin filaments. These are anisotropic to polarized light. The

H zone is in the center of the A band and only contains the myosin filaments. Refer to Figure 8 for the layout of the different regions of the muscle.

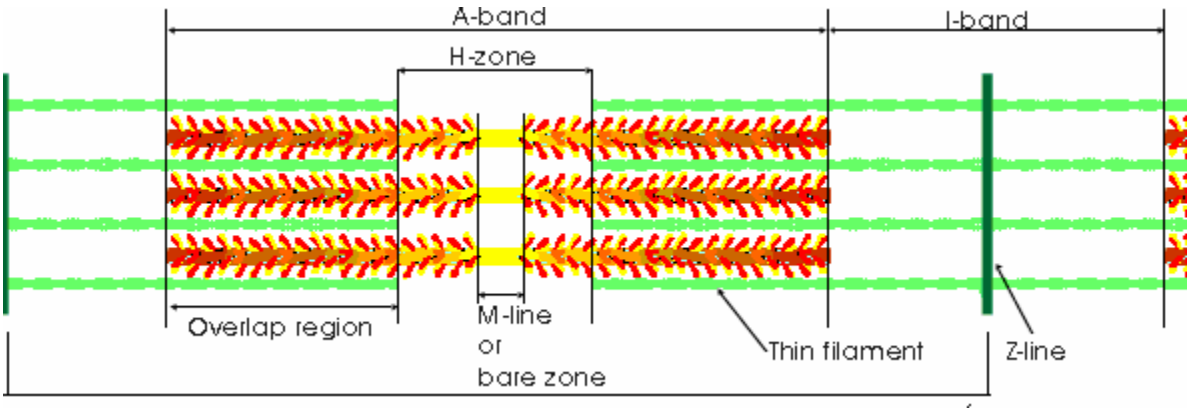

Figure 8. Various regions of the muscle.

3.0 PROCEDURE FOR EXPERIMENTATION

For the purpose of determining the optimum electrical characteristics required to stimulate muscle tissue, contractions and tissue damage of the gastrocnemius muscle were recorded and analyzed using ten Sprague-Dawley rats, weighing between 300 and 500 grams. Before surgery, the rats were anesthetized with ketamine and xylazine. Throughout the operation, the rats were frequently monitored for movement and withdrawal. In the surgery, an incision of 2 to 3 cm was made in the hind limb of the rat, exposing the biceps femoris. This muscle was divided, and sectioned, paralyzing the hind leg of the rat (see Figure 9). Once this was accomplished, a specialized device, placed in direct contact with the muscle, was used to stimulate the muscle and measure the muscle resistance.

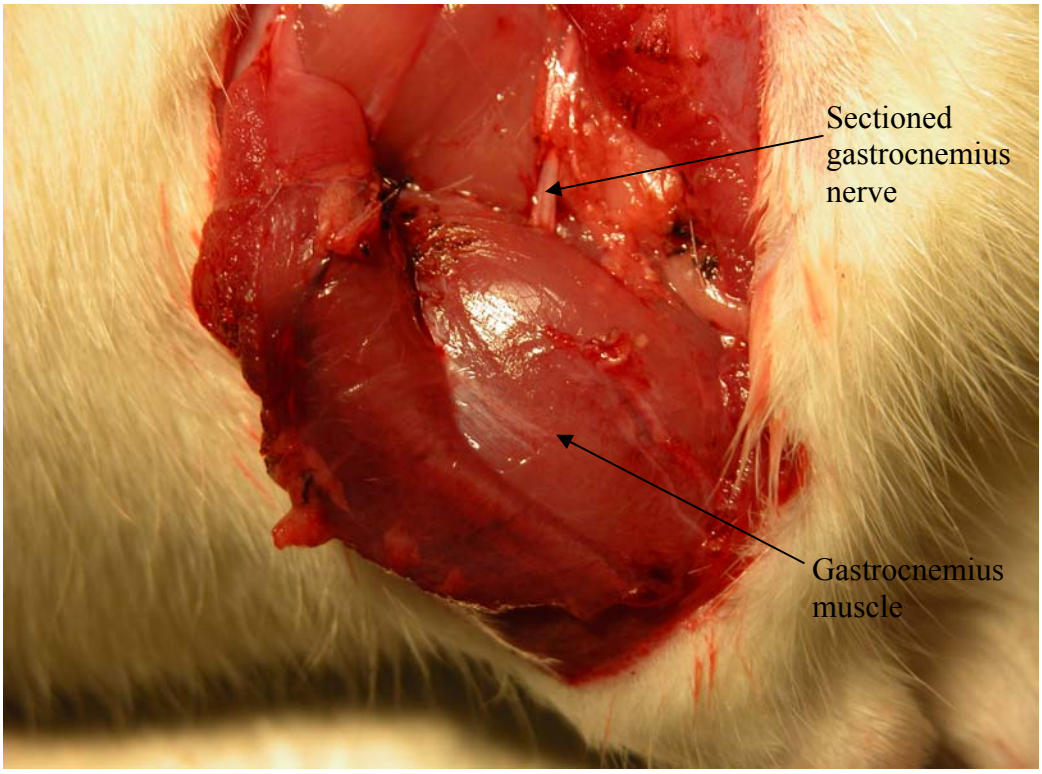

Figure 9. The gastrocnemius muscle and the gastrocnemius nerve in the hind leg of a rat (biceps femoris muscle reflected).

The device utilized, commonly referred to as the Mass Immunization Device (MID) was originally developed for performing electroporation and injecting DNA vaccines into muscle tissue. The device has several capabilities that were useful for the intended purpose of this project. Briefly, the device consists of a syringe cartridge and a hand held injection system. The cartridge provides a compartment for two syringes that expose only their needles. These needles serve as electrodes for a current to pass into the muscle tissue. Once the syringes are inserted, the cartridge is positioned in place into the injection system. The injection system has the capability of adjusting the voltage, the electrical pulse width, and electrical pulse count. The

variable constraints on this device are 30 to 80 volts for the voltage, 10 to 50 milliseconds for the pulse width and 1 to 10 pulses.

The experimental procedure for the device proceeds as follows. After the system was set to the desired parameters, an LCD screen indicated that the process was ready to begin. A standby button was then pressed which activates a loop to measure the initial resistance across the two needles. When the needles were inserted into the muscle tissue, the muscle resistance was recorded and displayed on the screen. An injection button was then pressed to activate the electrical stimulus that was programmed. When the electrical stimulus was applied, the muscle contracted if the electrical field strength was sufficient. As the muscle contracts, the device records the resistances measured before and after each stimulus. When completed, the injector retracted the needles and the resistances were displayed. Figure 10 provides an illustration of the device used.

A table of parameters was designed for the specific tests that were executed (see Table 1). The experiments used a constant pulse count of four, which signifies four blinks of an eye, while varying the current and pulse width. The current ranged from 0.005 milliamps to 37.3 milliamps. The pulse width, or the duration of each pulse, was set at 10 milliseconds. Once the series of tests were established, each trial was tested by placing the two needles directly into the gastrocnemius muscle and parallel to the muscle fibers. With each electrical pulse, the muscle contracts and the resistance of the muscle was registered in LabVIEW during each contraction. The current values were then recorded in Table 1 along with the severity of muscle contraction for each trial.

Table 1. Current values and type of contraction.

Current (mA)	Response	Current (mA)	Response	Current (mA)	Response
0.005	No visual contraction and no burning	3.0	Hard contraction and no burning	8.3	Hard contraction and no burning
0.01	Localized twitch/ contraction and no burning	3.3	Hard contraction and no burning	8.7	Hard contraction
0.015	Minimal contraction and no burning	3.7	Hard contraction and no burning	9.0	Hard contraction
0.02	Minimal contraction and no burning	4.0	Hard contraction and no burning	9.2	Hard contraction
1.0	Gentle contraction and no burning	4.3	Hard contraction and no burning	9.7	Maximal contraction and burning
1.5	Gentle contraction and no burning	4.7	Hard contraction and no burning	10.0	Maximal contraction and visual burning
2.0	Moderate contraction and no burning	5.0	Hard contraction and no burning	11.0	Maximal contraction and visual burning
2.1	Moderate contraction and no burning	5.3	Hard contraction and no burning	17.0	Maximal contraction and visual burning
2.2	Moderate contraction and no burning	5.7	Hard contraction and no burning	18.0	Maximal contraction and visual burning
2.3	Moderate contraction and no burning	6.0	Hard contraction and no burning	19.5	Maximal contraction and visual burning
2.4	Moderate contraction and no burning	6.2	Hard contraction and no burning	20.5	Maximal contraction and visual burning
2.5	Hard contraction and no burning	6.7	Hard contraction and no burning	21.5	Maximal contraction and visual burning
2.6	Hard contraction and no burning	7.0	Hard contraction and no burning	37.5	Maximal contraction and visual burning
2.7	Hard contraction and no burning	7.3	Hard contraction and no burning	37.5	Maximal contraction and visual burning
2.8	Hard contraction and no burning	7.5	Hard contraction and no burning		
2.9	Hard contraction and no burning	8.0	Hard contraction and no burning		

After each trial, a surgical marker was used to demarcate the area of tissue that was tested. These markers allowed the maximum amount of muscle to be utilized. An average of 3 trials per limb were done. With the completion of these tests, the rat was sacrificed in a carbon dioxide chamber and samples of the tissue were sectioned and analyzed under a microscope for damage using standard histologic techniques and categorized accordingly. Muscle tissue was then categorized into four groups signifying no response, contraction with no tissue burning, contraction with tissue burning and tissue burning. It should be noted that one leg muscle of a single rat was used as a control and not subjected to testing. With the results from the dissected muscle, an optimal range of current can be determined for muscle stimulation.

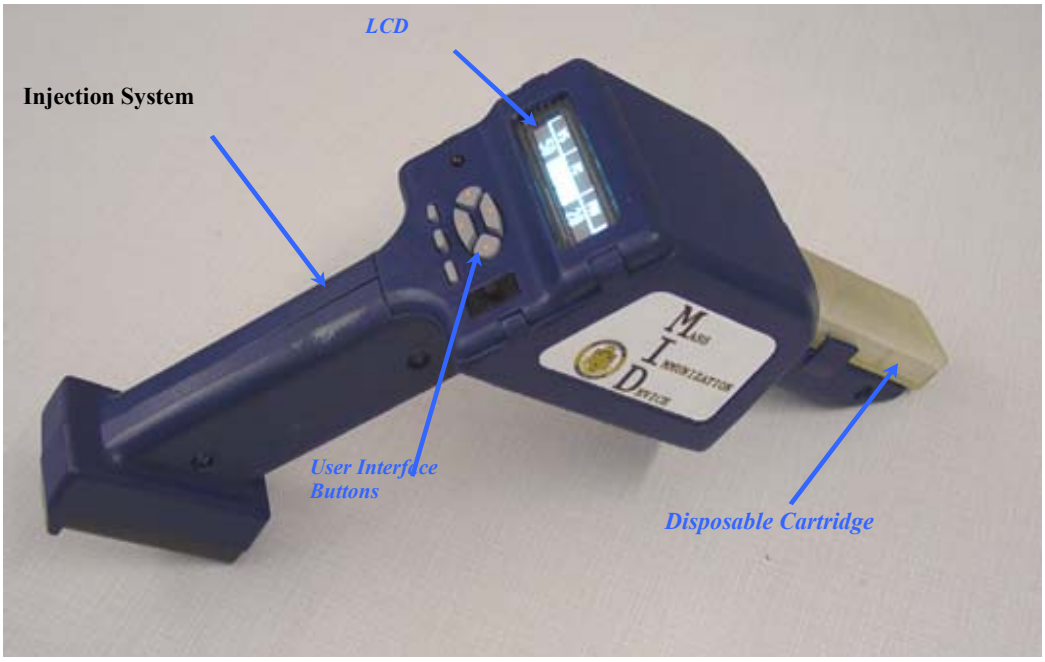

Figure 10. The Mass Immunization Device or the electroporation device.

In this section a detailed description of the Mass Immunization Device utilized in the experiments will be given. The driving mechanism in the Mass Immunization Device is a programmable integrated circuit (PIC). A digital potentiometer changes a signal from the PIC to an equivalent resistance. The keypad allows the user to input the settings on the Mass Immunization Device, while the LCD displays the entered information and the resistance after each pulse. Two voltage limiters are used to control the voltage of the battery used in the device. A voltage booster is also used to increase the voltage to obtain the range for the device. The pulsing and the resistance measure are done with two solid-state relays and the needles serve as electrodes to pass the current through the muscle.

The PIC in the Mass Immunization Device sends a digital signal to move up or down and a pulse from 1 to 100 to a digital potentiometer. The potentiometer then converts this signal to a resistance value from 10 to 1000 Ohms. (1 pulse =10 Ohms). Incorporated in the circuit is a voltage limiter that is attached to the potentiometer. The voltage limiter regulates the voltage by the resistance designated on the potentiometer. This voltage can be from 2 to 6.5 Volts. A voltage booster is also used and increases the voltage from 30 to 80 Volts, so the user can input the desired voltage on the device. From this, a solid-state relay is used to activate pulsing on the device. Another solid-state relay is used to measure the tissue resistance. In order to measure this resistance, a voltage divider circuit is used. First, a resistance of known value is placed in the circuit and its voltage is measured (from 0 to 5 Volts) and is input into the PIC. Using this voltage along with the voltage supplied to the PIC, the tissue resistance can be calculated, using the voltage divider equation. The Figure 11 below shows the flow diagram of how the Mass Immunization Device operates.

To initiate the pulse, the number of pulses and the pulse width are set. Just before the pulse begins, the voltage is set at 0 Volts for a certain length of time. When the injection button on the device is pressed, the relay for high voltage pulsing turns on, and the pulse begins (1-10) at the voltage selected by the user (30-80V) and continues for the time (10-50 ms), indicated by the pulse width, on the device. At the end of this pulse, the high voltage pulsing relay is turned off and the voltage decreases to 5 Volts. Then the resistance-measuring relay is turned on and the resistance of the tissue between the two needles is measured (via voltage divider circuit) and displayed on the screen of the device. The second relay is turned off and the voltage further decreases to 0 Volts until the next pulse begins. This continues until all the pulses indicated on the device have completed.

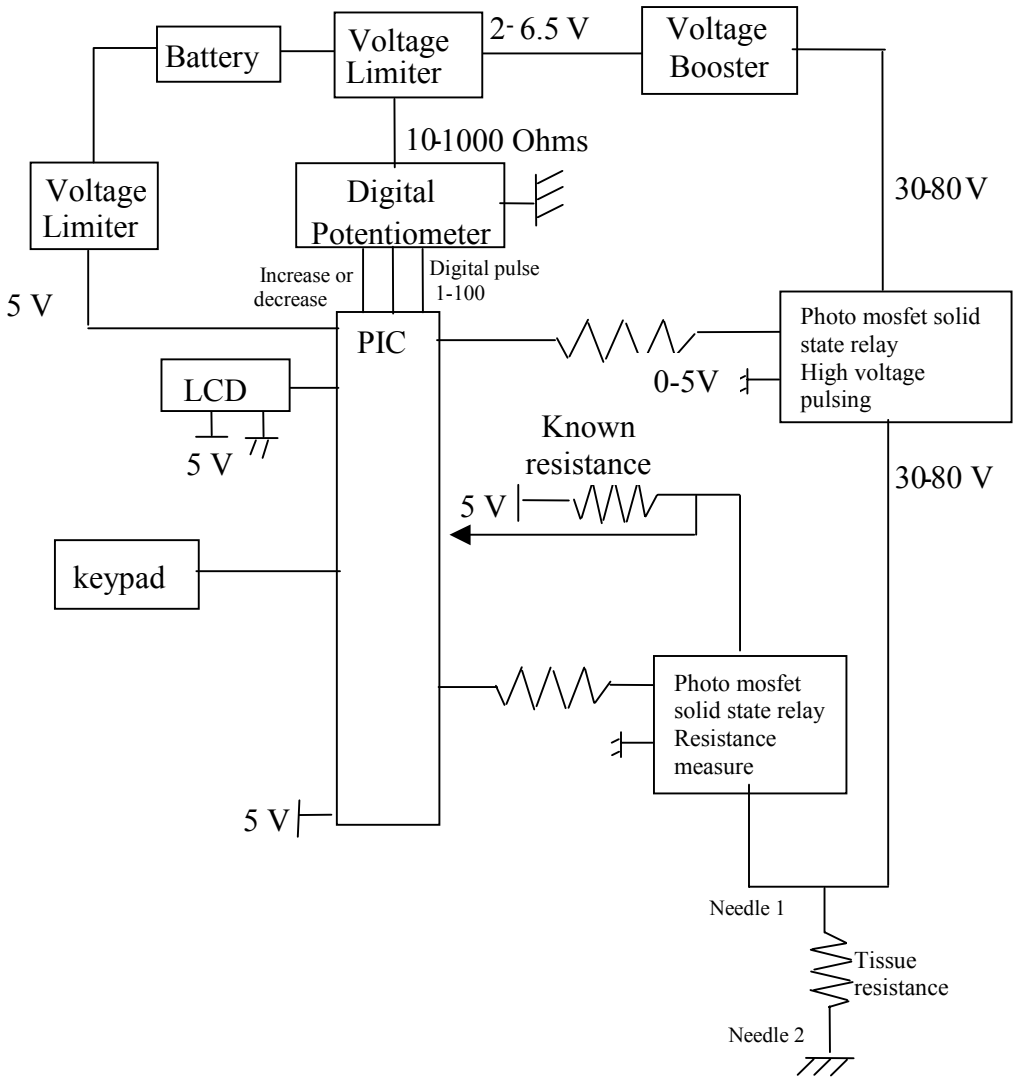

Figure 11. Circuitry for the Mass Immunization Device.

In order for the Mass Immunization Device to calculate the resistance, a trend line was developed representing resistance versus voltage. To develop this trend line, a decade box and a resistor of known value were set up using a voltage divider circuit (see Figure 12). The voltage was measured across the decade box for different value of resistance. These voltages were then plotted against the resistance on the decade box and a line of best fit was determined. A third

order polynomial equation best represented the trend line. However, at higher resistance values, greater than 15 KOhms, the equation did not accurately fit the data. Therefore, resistance values above 15 KOhms were thought to be inaccurate and displayed as infinite.

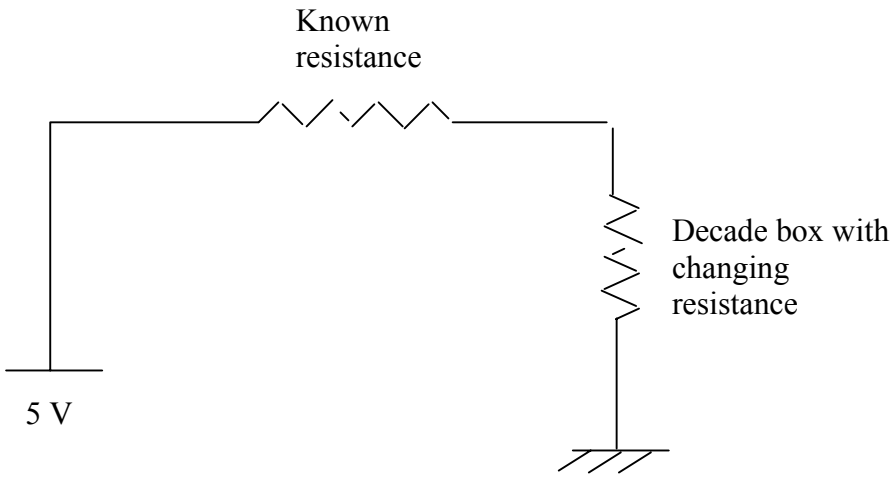

Figure 12. Voltage divider circuit used to establish trend line.

This Mass Immunization Device was later modified to allow for an input of constant current in the muscle contraction experiments. A circuit was designed and incorporated into the device to enable regulation of the current applied to the muscle tissue (see Figure 13).

When the Mass Immunization Device is in use, the current from the device travels through a current limiting chip in the circuit. This chip limits the current going into the circuit, based on the amount of current the user wants to go through the tissue. A Data Acquisition (DAQ) Board is connected to the circuit and to LabVIEW. LabVIEW is a virtual instrument that uses icons to create a program. The program developed for this project was constructed for the Mass Immunization Device to calculate and record the muscle tissue resistance. The LabVIEW code is set up as follows. In the front panel of the LabVIEW display, three resistances are

entered, R1, R2 and R3. R1 and R2 are resistors in series, with a 10 to 1 ratio, connected in parallel with the muscle tissue in series with R3, a 1 KOhm resistor. The reason for the 10 to 1 ratio between R1 and R2 is so that most of the current traveling through the circuit goes through the muscle tissue and the 1 KOhm resistor. In order to determine the resistance through the muscle tissue, the DAQ board measures the voltage across R2 and uses a voltage divider to determine the total voltage across R1 and R2.

$$V_s = V_o\left(\frac{R1+R2}{R2}\right) \qquad (1)$$

Since the DAQ board can withstand values of up to 5 volts, the voltage divider is used to reduce the voltage from the device going into the DAQ board. The DAQ board also measures the voltage across R3, the 1 KOhm resistor. With these two voltages, $V_{R1,R2}$ and V_{R3}, the voltage across the tissue can be determined, V_t by subtracting $V_{R1,R2}$ from V_{R3}. Knowing the tissue voltage, the current input into the circuit can be used to obtain the tissue resistance,

$$V_t = V_{R1,R2} - V_{R3} \qquad (2)$$

$$R_t = \frac{V_t}{I_t} \qquad (3)$$

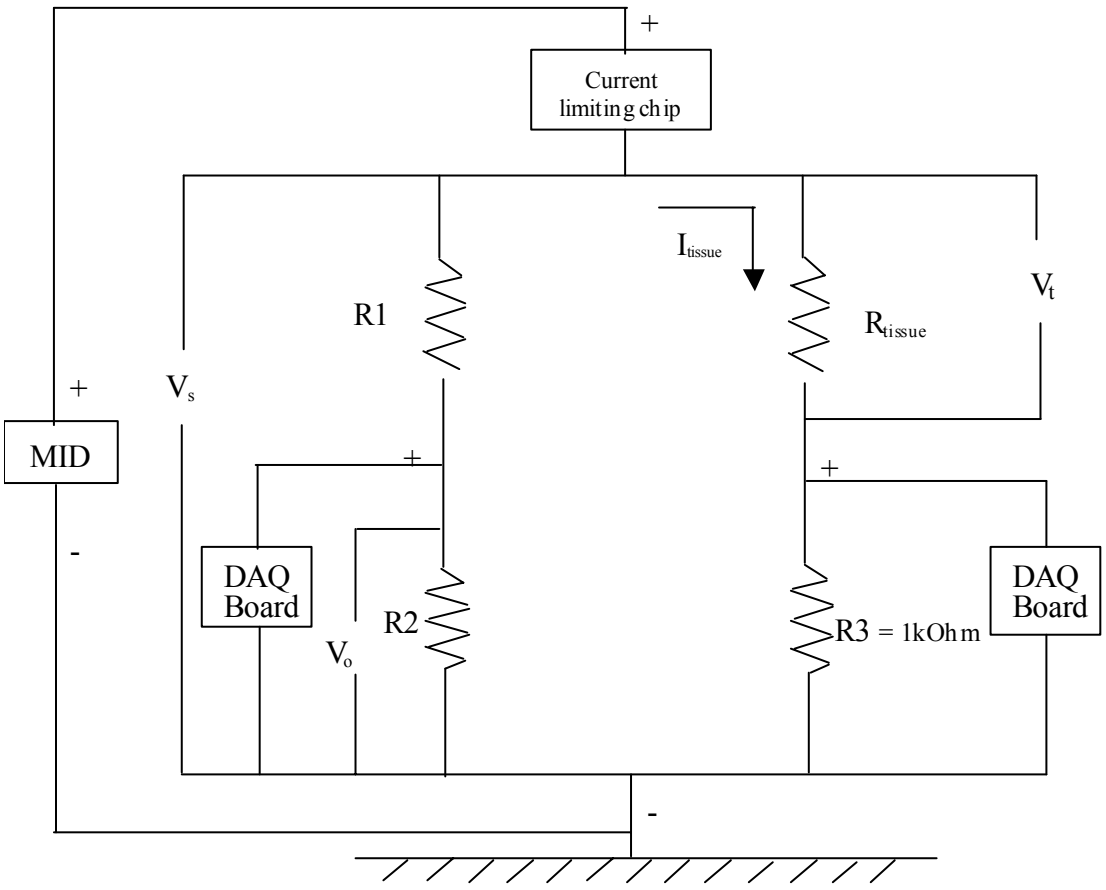

Figure 13. Circuitry for constant current.

4.0 RESULTS

The range of current that was tested is shown in Table 1. This wide range was chosen to ensure no muscle contraction for the lower limit and muscle contraction with burning for the upper limit. For the analysis of these results, it was assumed that all the rats have the exact genetic and chemical makeup.

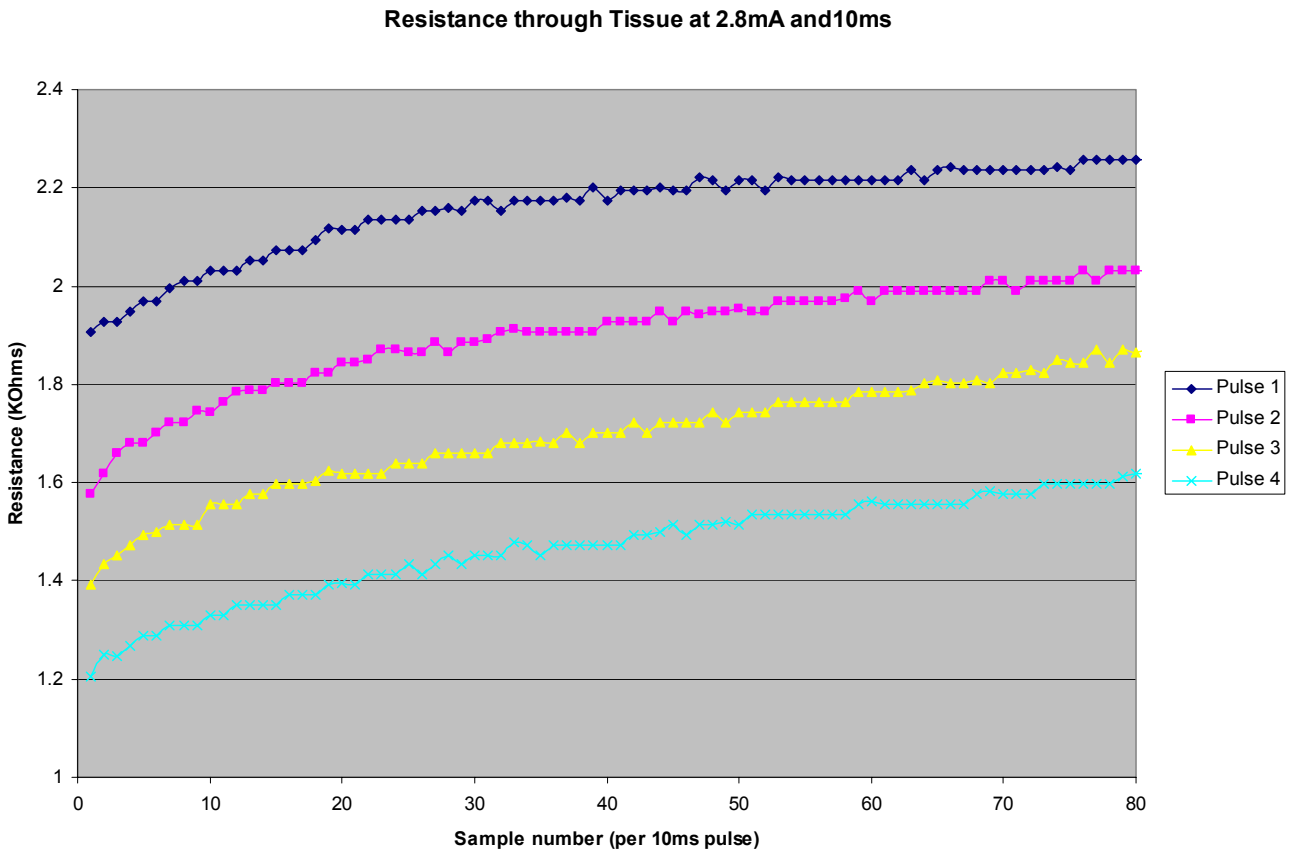

Figure 14. An example of capacitive behavior at 2.8mA and 10ms.

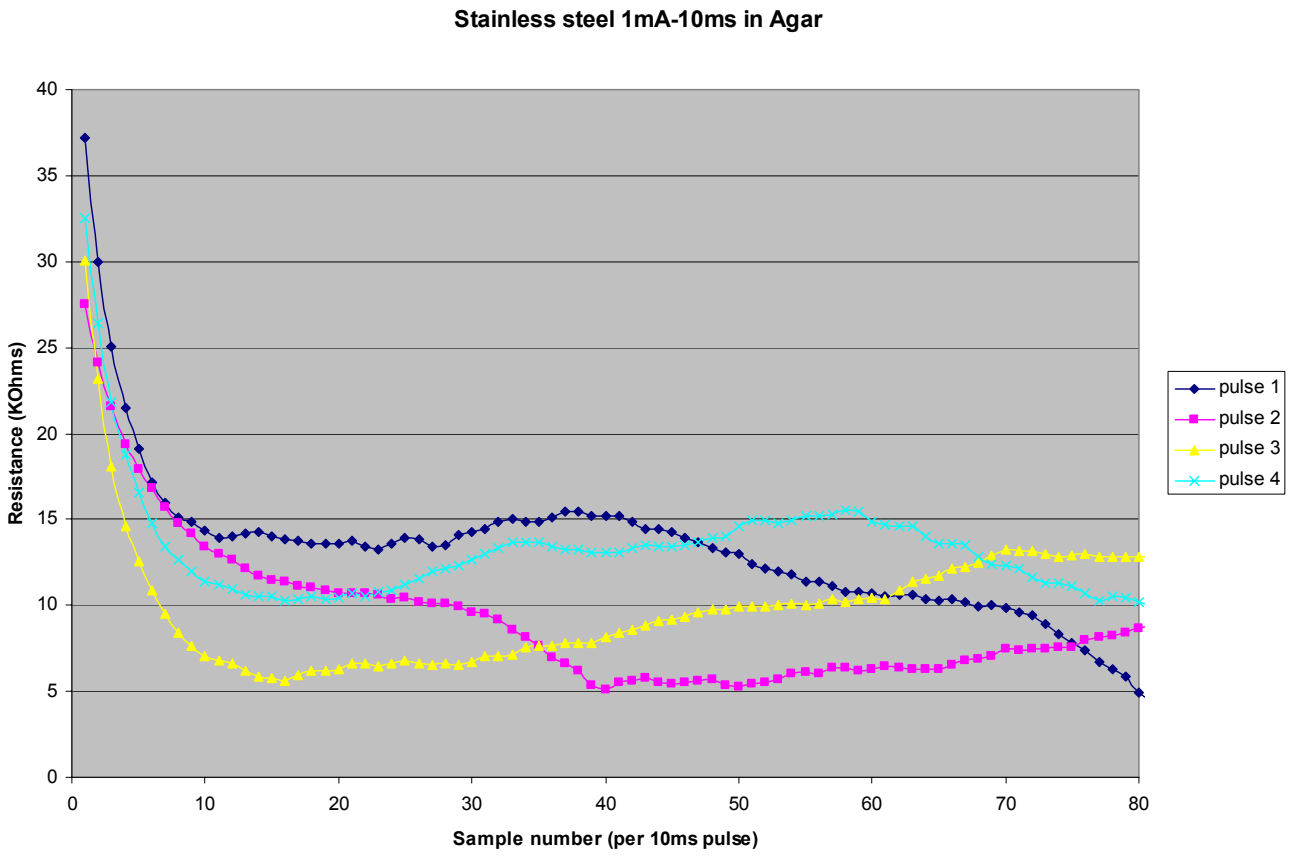

Figure 15. Stainless steel needles tested in agar at 1mA and 10ms.

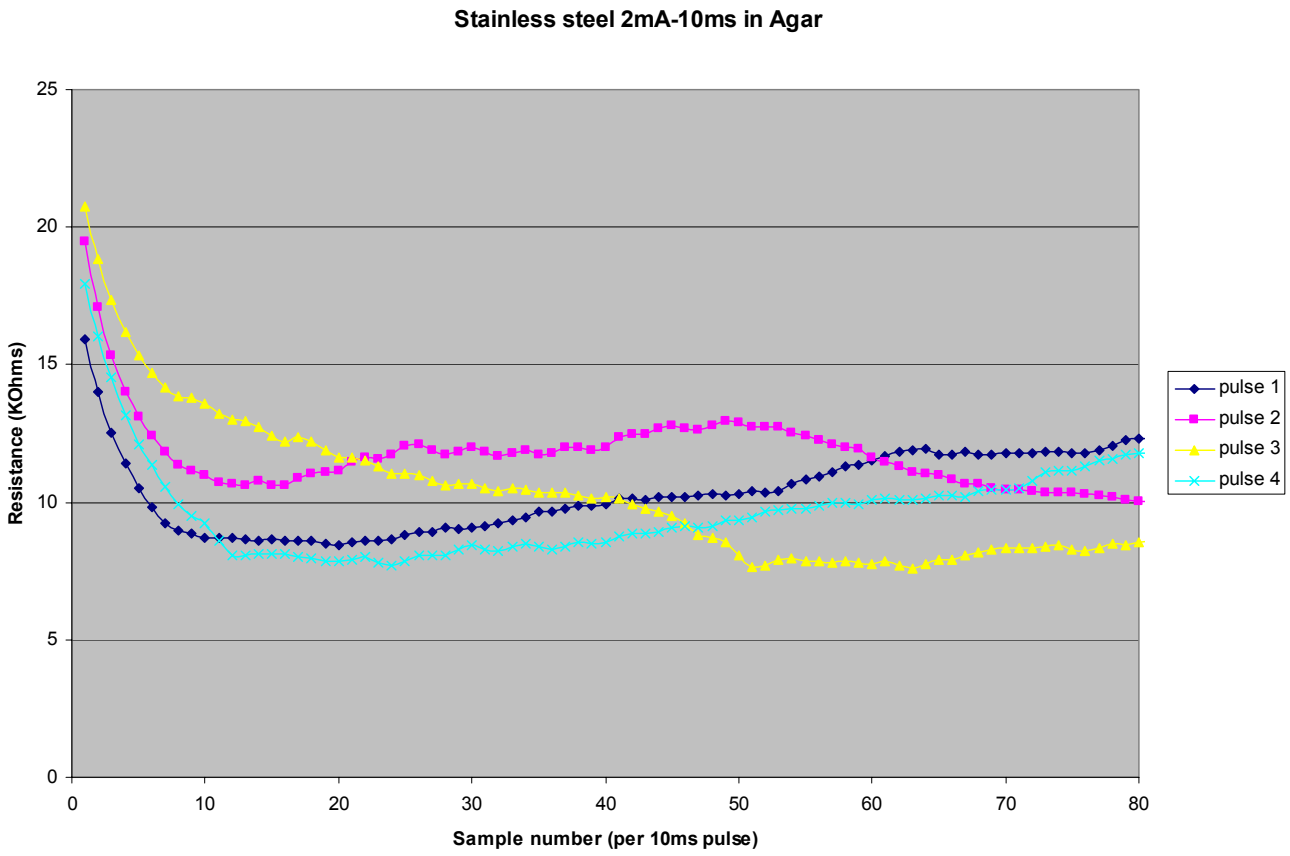

Figure 16. Stainless steel needles tested in agar at 2mA and 10ms.

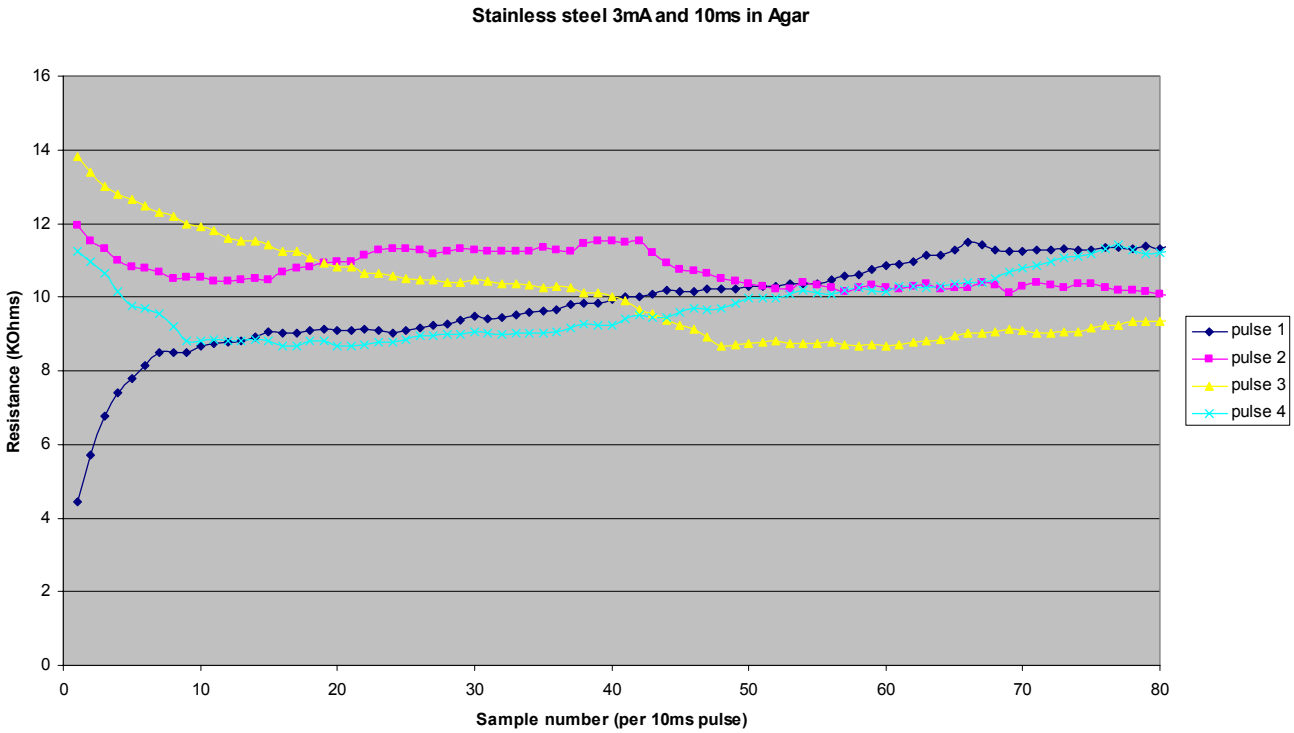

Figure 17. Stainless steel needles tested in agar at 3mA and 10ms.

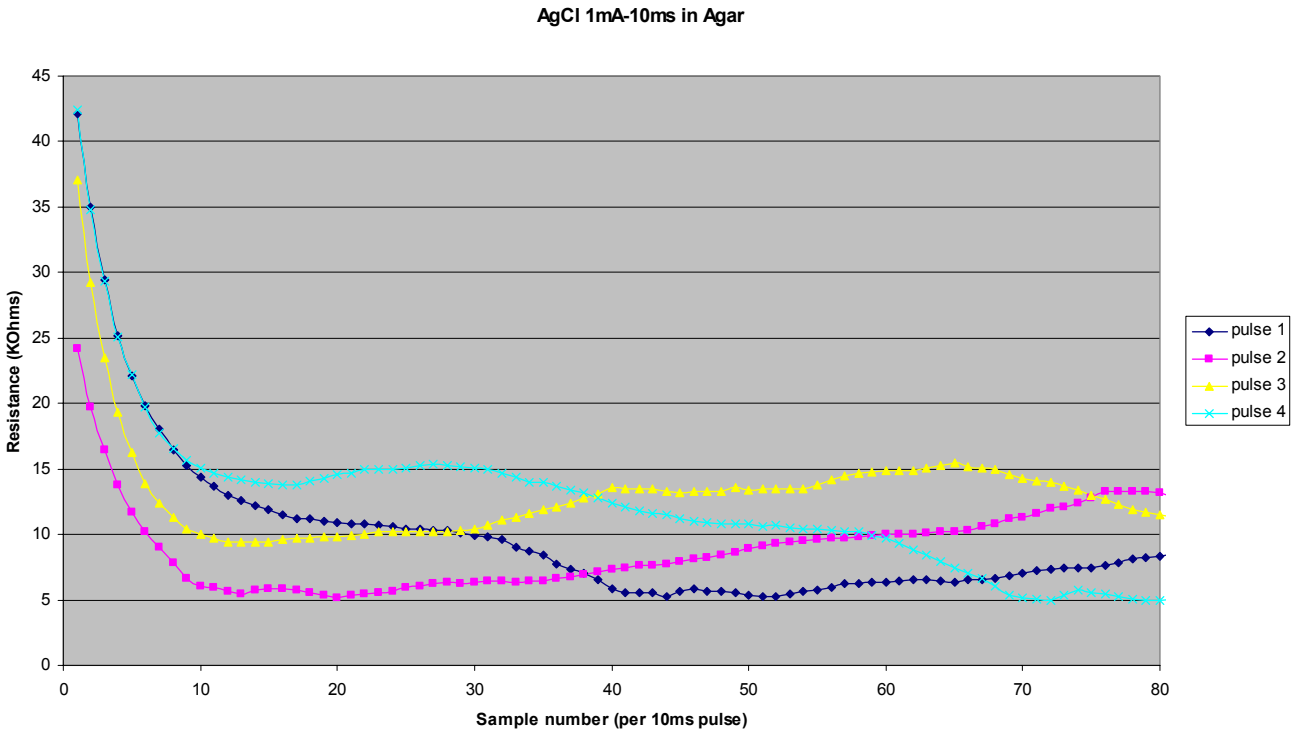

Figure 18. Silver chloride needles tested in agar at 1mA and 10ms.

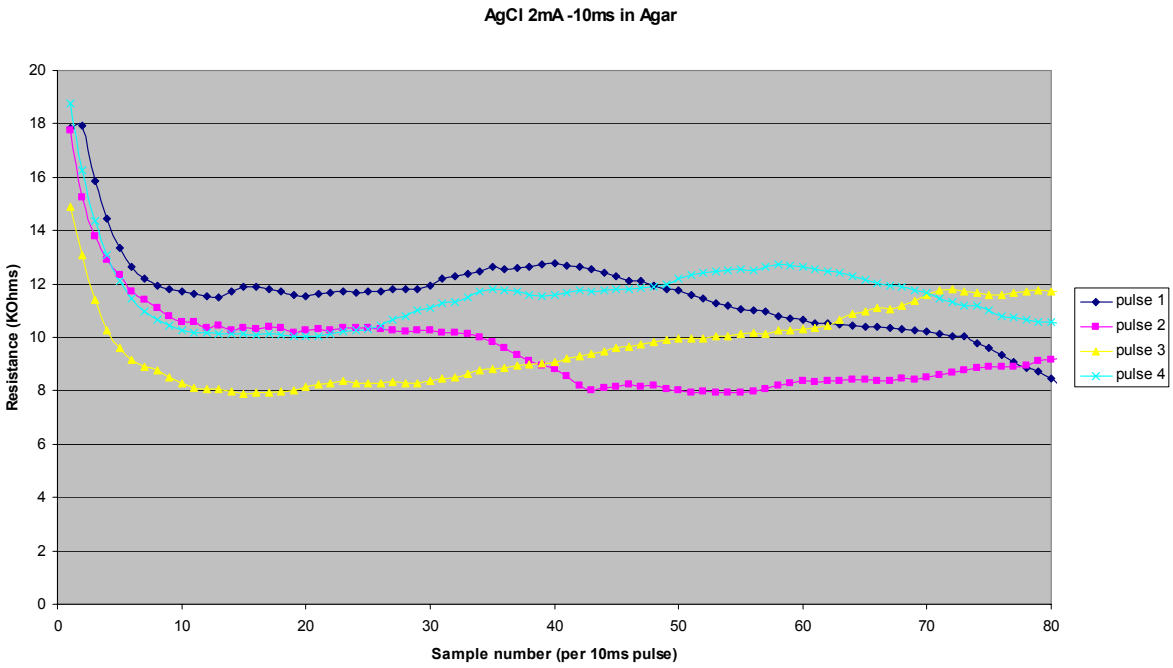

Figure 19. Silver chloride needles tested in agar at 2mA and 10ms.

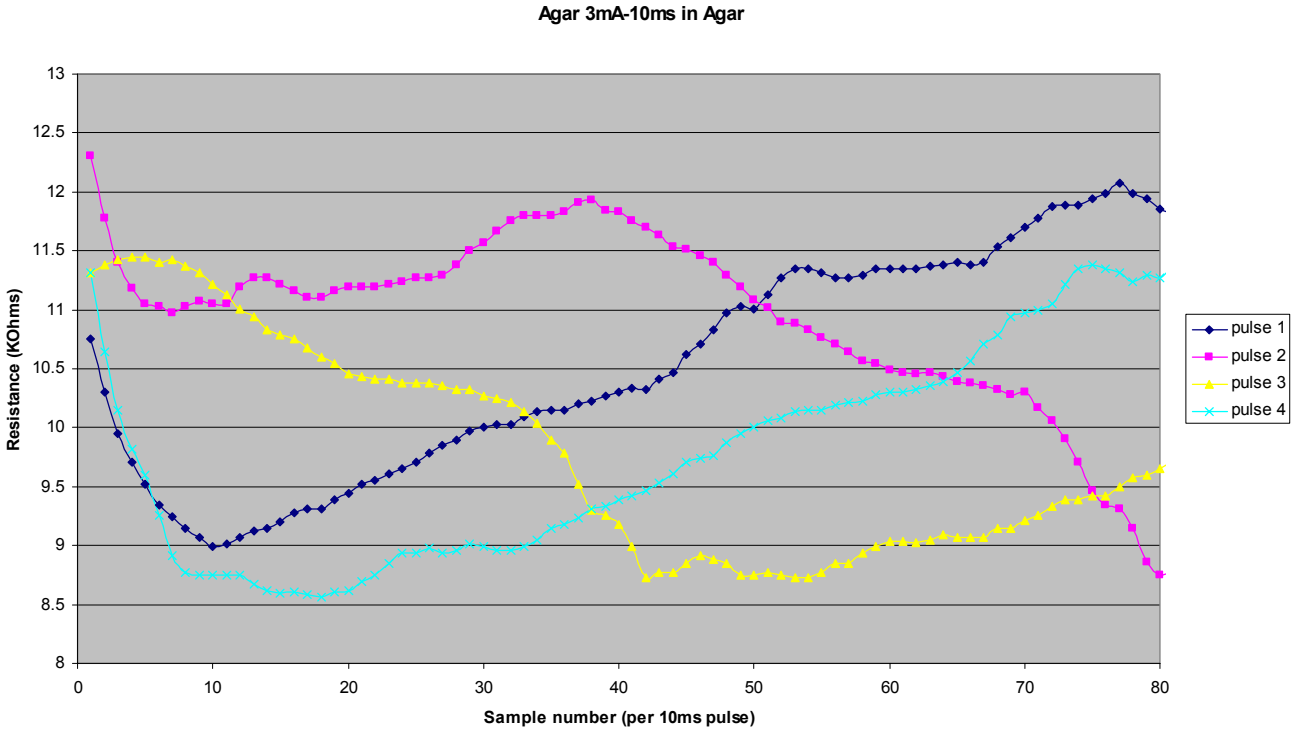

Figure 20. Silver chloride needles tested in agar at 3mA and 10ms.

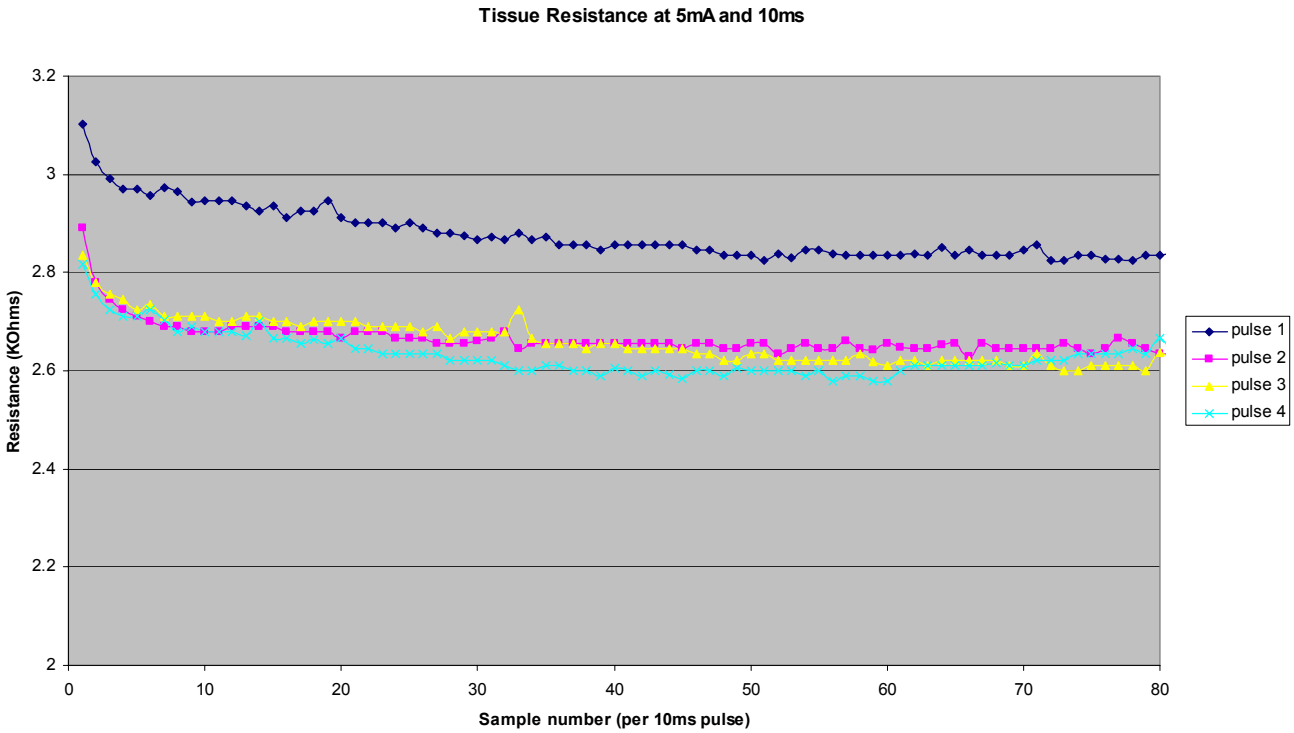

Figure 21. Non-capacitive behavior at 5mA and 10ms.

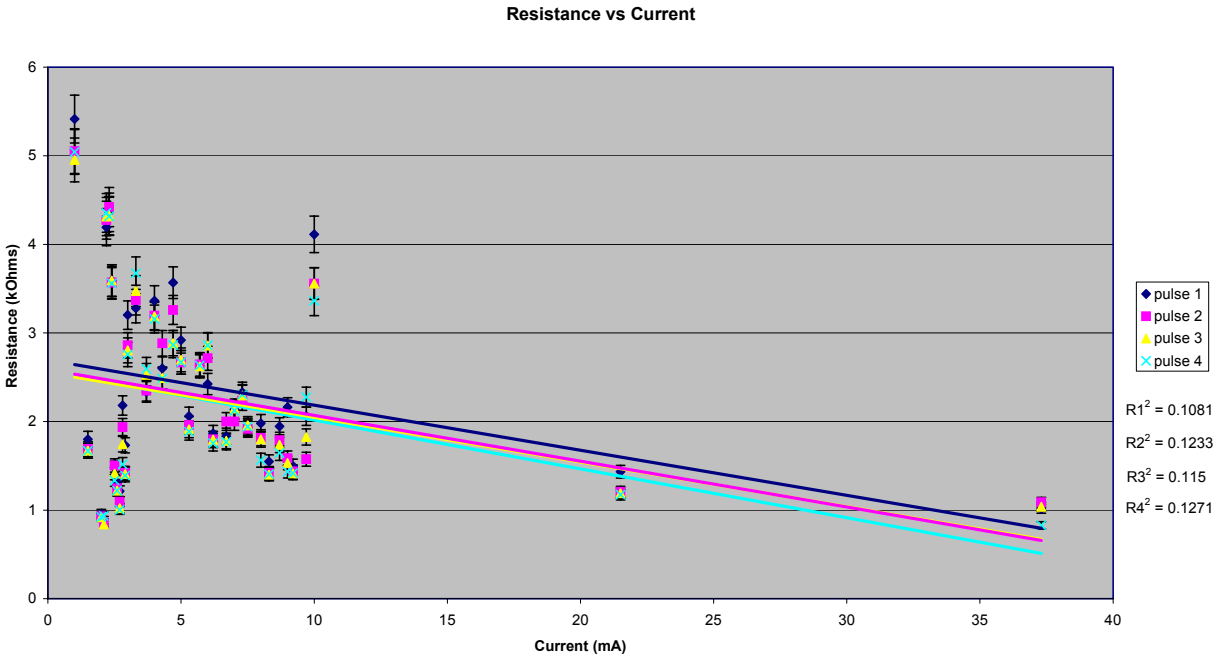

Figure 22. Complete data of resistance versus current in rat muscle.

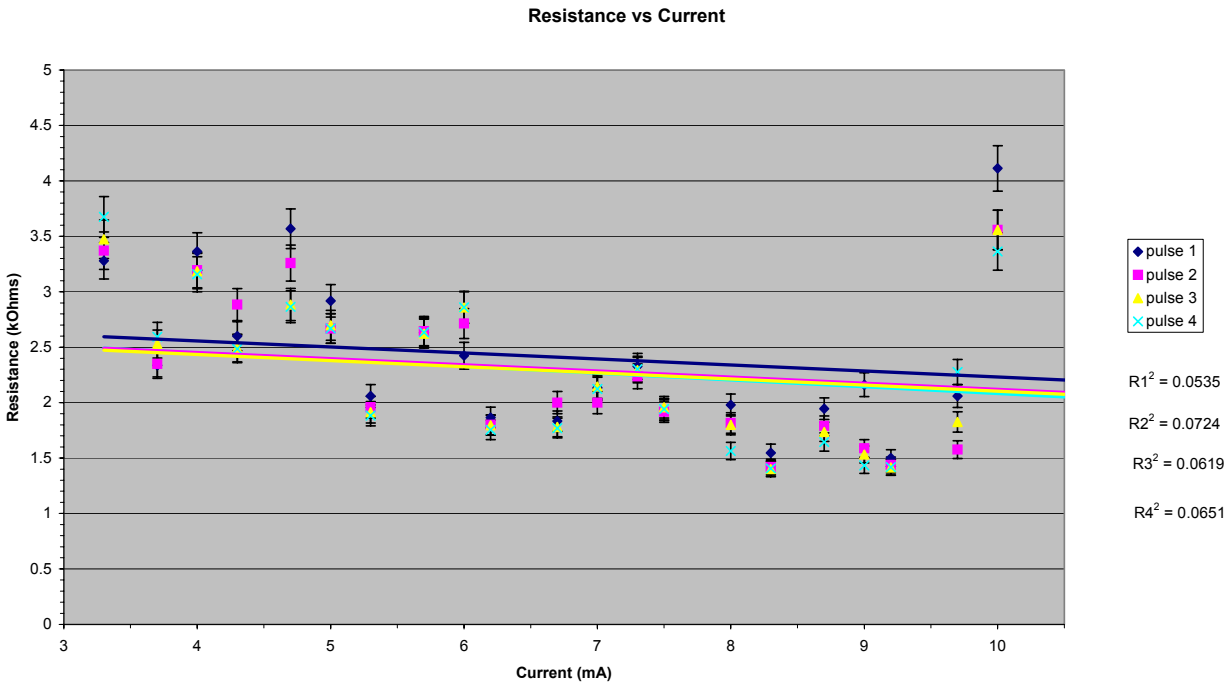

Figure 23. Resistance versus current from 3.3mA to 10mA.

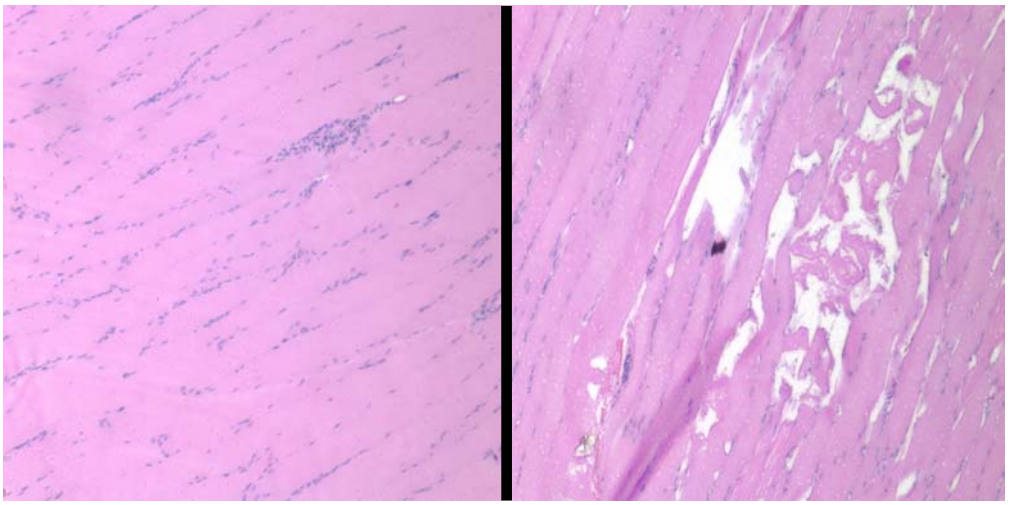

Figure 24. Healthy muscle tissue and coagulative necrosis in muscle tissue as a result of burning.

5.0 DISCUSSION OF RESULTS

From the results in Table 1, it appears that the range of current to stimulate muscle contraction without causing tissue burning is between 0.01 and 8.3 milliamps. After observing the strength of muscle contraction, currents in the region of 0.01 to 0.02 milliamps showed gentle contractions that were compatible with the movement required for an eye blink, based on a visual assessment.

An example of the typical behavior of the muscle tissue for currents from 1 to 3miliamps is characterized in Figure 14. The data depicts that the resistance may exhibit capacitive behavior since there is a logarithmic increase in the resistance. A possible explanation for why this behavior is occurring is that stainless steel needles were used for the electrodes to transport the current into the tissue. Since stainless steel is a poor conductor, the two electrodes may be acting as capacitors. Charge builds up on the ends of the needles until saturated then discharges. As a result, a series of tests were performed in conjunction with the rat testing to validate this theory [21].

5.1 STAINLESS STEEL AND SILVER CHLORIDE EXPERIMENTS

In order to determine if the capacitive behavior of the resistance was a result of the stainless steel needless, a sample test was done using two types of needles. Each test was performed in a gel like solution, representing physiological solution. First, agar (2gm

agar/100mL water) was mixed with salt water (0.9gm NaCl/100mL water) and heated, then allowed to cool to create a gel like solution that represented tissue. During this process, the current limiting circuit was connected to the Mass Immunization Device and LabVIEW, which recorded the voltage, current and resistance. The same conditions were used when testing with the agar, as with the rats. To acquire the general behavior of the resistance through the agar, only current values at 1, 2 and 3 milliamps were tested at a 10 millisecond pulse width.

The first of the two sets of tests were performed using stainless steel needles that were identical to those used in the rat experiments. After graphing the resistance of the agar (see Figures 15 through 17), the resistance nonlinearly decreases, but does not reach steady state over time, as was found for the resistance tested on the muscle. Therefore, the resistance of the agar does not depict capacitive behavior.

The next tests used sterling silver wire coated in Chlorine (Bleach) and were tested in the same manner. Since the silver chloride has ionization or charge carriers, it will continuously carry the current through the tissue, unlike the stainless steel. First, the silver wires were sanded and soaked in Bleach for 30 minutes until the wires turned black. The wires were then placed in the agar, similar to the previous experiment. Similar to the data from the stainless steel plots, it appears that the resistance nonlinearly decreases with time (see Figures 18 through 20). As expected, the resistance graphs do not exhibit capacitive behavior.

With the information obtained from the agar test, no trends were established to further understand the data acquired from the rat testing. Both the stainless steel needles and the silver chloride needles exhibit a decrease in resistance. This indicates that there was no charge built at the tips. However, if the stainless steel needles did cause a charge build up, a contraction of the

muscle was still produced. This may have been a result of the potential difference between the membranes that caused the flow of ions, thus resulting in a contraction.

At currents above 3 milliamps, the muscle resistance did not exhibit capacitive behavior. An example of this is shown in Figure 21. The tests conducted below 3 milliamps displayed a trend of increasing resistance, unlike the tests conducted beyond 3 milliamps. It is thought that the current applied to the muscle was low enough for the muscle to attempt to restore itself to its initial resistance before stimulation. Since the data generated from this test did not follow the trends for larger current values, these current levels have created outliers and were therefore discarded.

5.2 BEHAVIOR OF RAT TISSUE

Figure 22 shows the complete set of data obtained from the rat testing. For trials from 11 to 20.5 milliamps, LabVIEW displayed a current supply of only 10 milliamps. For these tests, an average of the resistance for each pulse was taken and presented at 10 milliamps. Therefore, the concentration of this discussion will revolve around data points up to 10 milliamps, shown in Figure 23.

In general, the data collected from the rat testing revealed that the resistance in the muscle slightly decreased after each consecutive pulse during electrical stimulation (see Figure 23). A possible hypothesis would be that damaged tissue possesses a lower electrical resistance than healthy tissue. Damage would tend to break down membranes, which are the high-resistance portion of most tissue; the extra-cellular and intracellular solutions have mobile ions and therefore have lower resistance. Mechanical damage to the tissue of the rat gastrocnemius

muscle initially occurs when the needles are directly placed into the muscle. Further damage is caused by the combination of the pulses generated by the Mass Immunization Device and the muscle contracting. This combination may cause a wider gap where the needles are inserted and create more tissue damage. Since the resistance is decreased with each successive pulse, the current is forced to take a path of lower resistance, possibly through interstitial fluid. Interstitial fluid is the fluid surrounding living cells. It is comprised of mobile ions in water that enables conduction.

The graph in Figure 23 also shows that the resistance is greatest during the first pulse and then decreases for the 2^{nd}, 3^{rd} and 4^{th} pulse. The latter three pulses reduce to nearly the same resistance values. This might be because after the first pulse, the tissue is maximally damaged and therefore the resistance remains constant during the last three pulses.

Recall when an action potential occurs by electrical stimulation, the potential across the membrane decreases. The negative current from the electrode decreases the voltage on the outside of the membrane to a negative value nearer to the voltage of the negative potential on the inside of the fiber. This decrease in membrane potential causes the opening of the sodium channels, allowing positive sodium ions to flow into the membrane, resulting in a more positive potential on the membrane interior. Given that the membrane is accepting oppositely charged ions, this may also cause the membrane to become less resistant to current.

Figure 23 shows how the muscle resistance is inversely proportional to the current. In order to achieve higher current levels, an increase in voltage is required. It is thought that the higher resistances at the lower currents are due to the lower voltages.

With each trial at different current levels, it was observed that the initial tissue resistance varied. This can be a factor of distance between the needles when inserted into the muscle. The initial resistance of the muscle increases the farther apart the needles are placed into the muscle.

The preferable amperage to stimulate muscle contraction for the eye is in the range of 0.01 and 0.02 milliamps, where the muscle exhibited localized contraction. However, for these current levels, the resistance recorded by LabVIEW, between 0.01 and 0.02 milliamps, displayed an infinite value. This was based on the criteria in the LabVIEW program that current levels less than 0.10 milliamps are displayed as infinite resistance. The 0.10 milliamps was arbitrarily chosen. It was thought that this value would filter out inaccurate data. Recall the trend line that was developed to calculate the resistance**.** The values between 1 and 15 KOhms follow the trend line and are more accurate than values greater than 15 KOhms. When the value in LabVIEW was changed to less than 0.10 milliamps, the resistance of the tissue reaches values beyond 15 KOhms. Since these values fall outside of the trend line, the data is considered unreliable. Refer to Appendix B for plots of the lower current levels.

6.0 CONCLUSION

From the rat experiments, it was shown that the optimal current range is between 0.01 and 8.3 milliamps. For this particular application, the preferred current levels are in the milliamp region (0.01 – 0.02 milliamps).

It was thought that the stainless steel needles that were used from the 1 to 3 milliamp tests displayed capacitive behavior. However, the supplemental experiment, using silver chloride needles, did not prove the initial theory that stainless steel needles used for rat testing showed capacitive characteristics. For the rat experiments, the resistance was observed to decrease with each consecutive pulse and with increasing current. This decrease in resistance is due in part to damaged tissue from a combination of the inserted needles and the electric pulses. The current then passes through the interstitial fluid, a path of lower resistance. Another possible reason for the decrease in resistance is that the membrane is then permeable to positively charged ions, which may also cause it to become less resistant to current flow. It was also noted that as the current increases, the voltage is also increased and it becomes easier to traverse layers of muscle tissue, therefore decreasing the resistance.

7.0 FUTURE WORK

Although the range of current has been determined, the current levels in the microamp region display a slight amount of noise and do not distribute a steady current throughout the pulse (see Appendix C). This may have been due to the current limiting chip used in the circuit. It is a possibility that the chip is not sensitive enough to handle such small current levels. Therefore, lower currents may have to be retested with a more sensitive chip for a more accurate reading, since the muscle may have been stimulated at a slightly higher current than expected. In addition, currents near the upper limit of this range may not be used for this application; however, the three tissue samples between 8.3 and 9.7 milliamps can be examined to ensure that 8.3 milliamps is the maximum value. If necessary, smaller increments of current can be tested as well.

Even though burning does not occur within the determined limit, it should be noted that some current values within this range are painful when applied to the skin and may cause burning after long periods of time. Therefore, further investigation is necessary to determine whether currents in this portion of the range are suitable for optimal muscle stimulation with regard to an eye blink. Studies indicate that a person blinks 24 times a minute, on average [23]. Since this device will require a constant application of current, the current may gradually cause burning of tissue over a significant period of time. In order to detect if this is occurring, tests can be performed in which a current is applied several times a minute for an extended period of time.

If this is still occurring, using a lower pulse width, which will also reduce any existing pain, may have to be considered. Figure 24 compares burned tissue with healthy tissue.

Currently, tests to establish signaling between a denervated rat leg and a healthy rat leg are being performed.

APPENDICES

APPENDIX A

Damaged Tissue Data

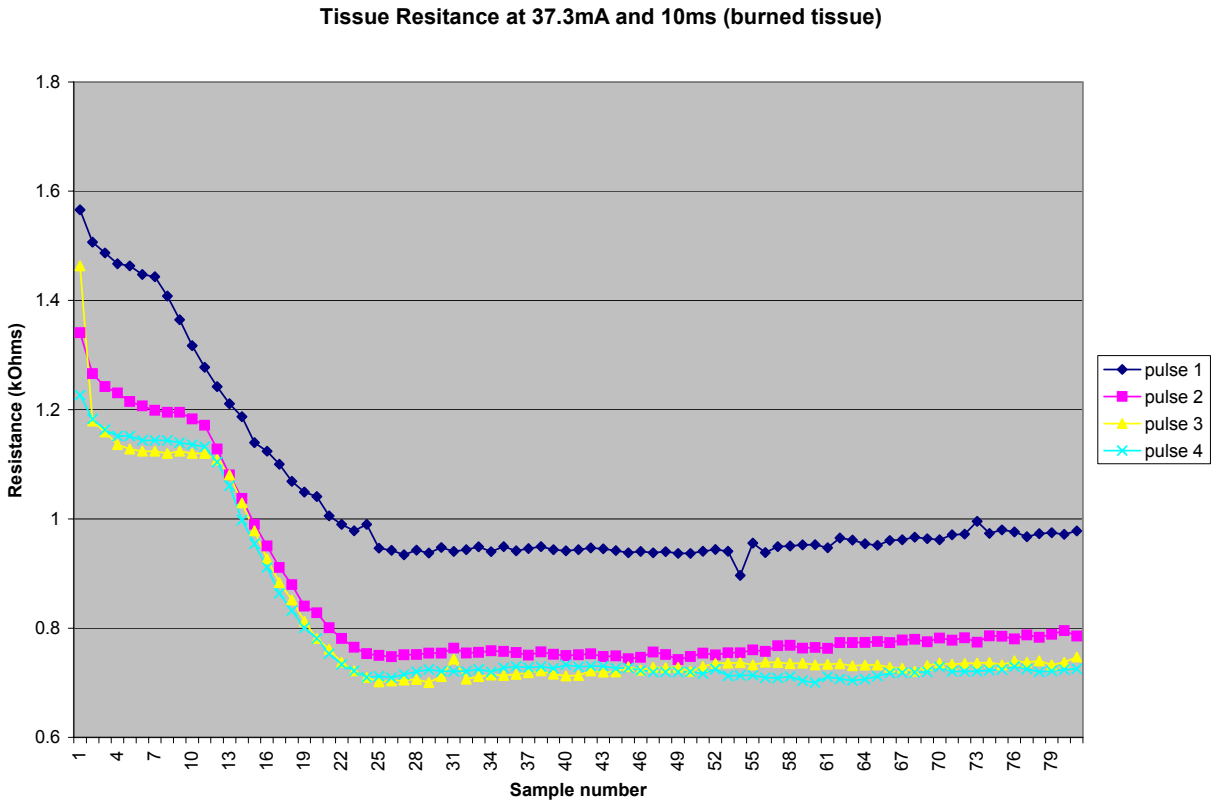

APPENDIX B

Tissue resistance for current below 1 milliamp

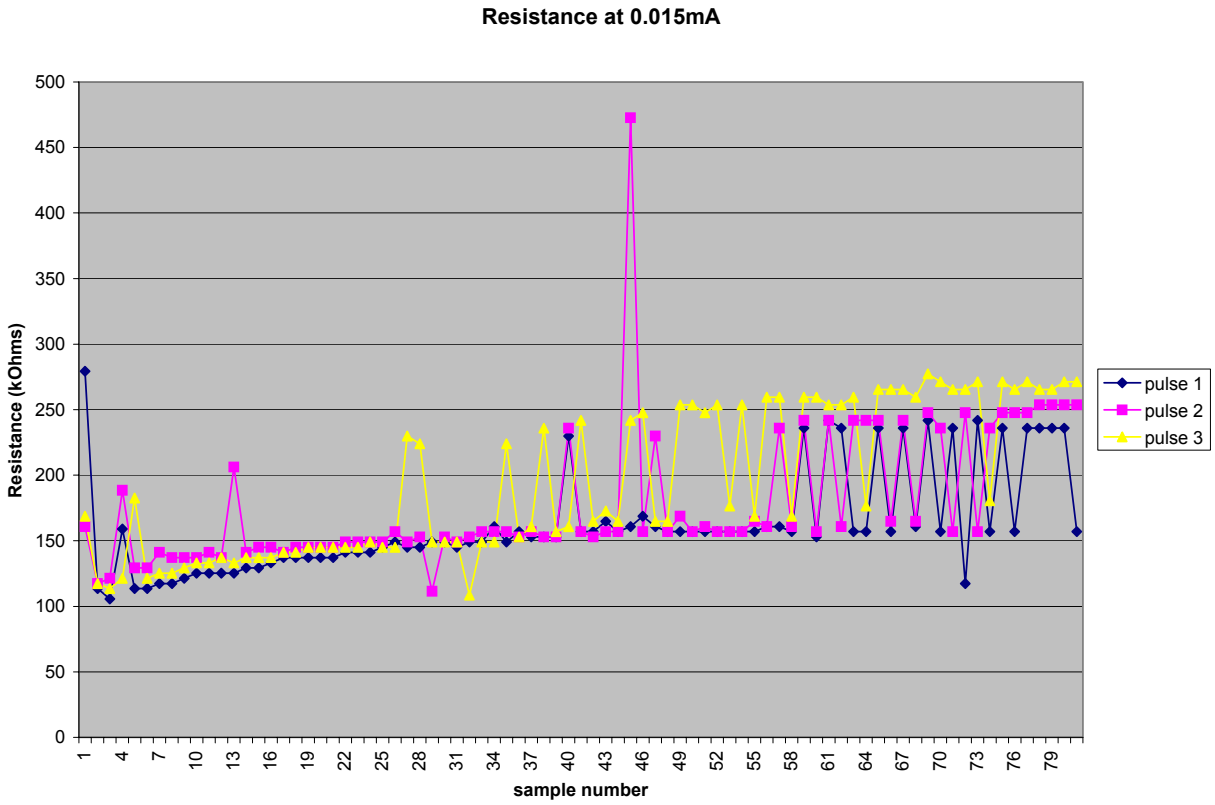

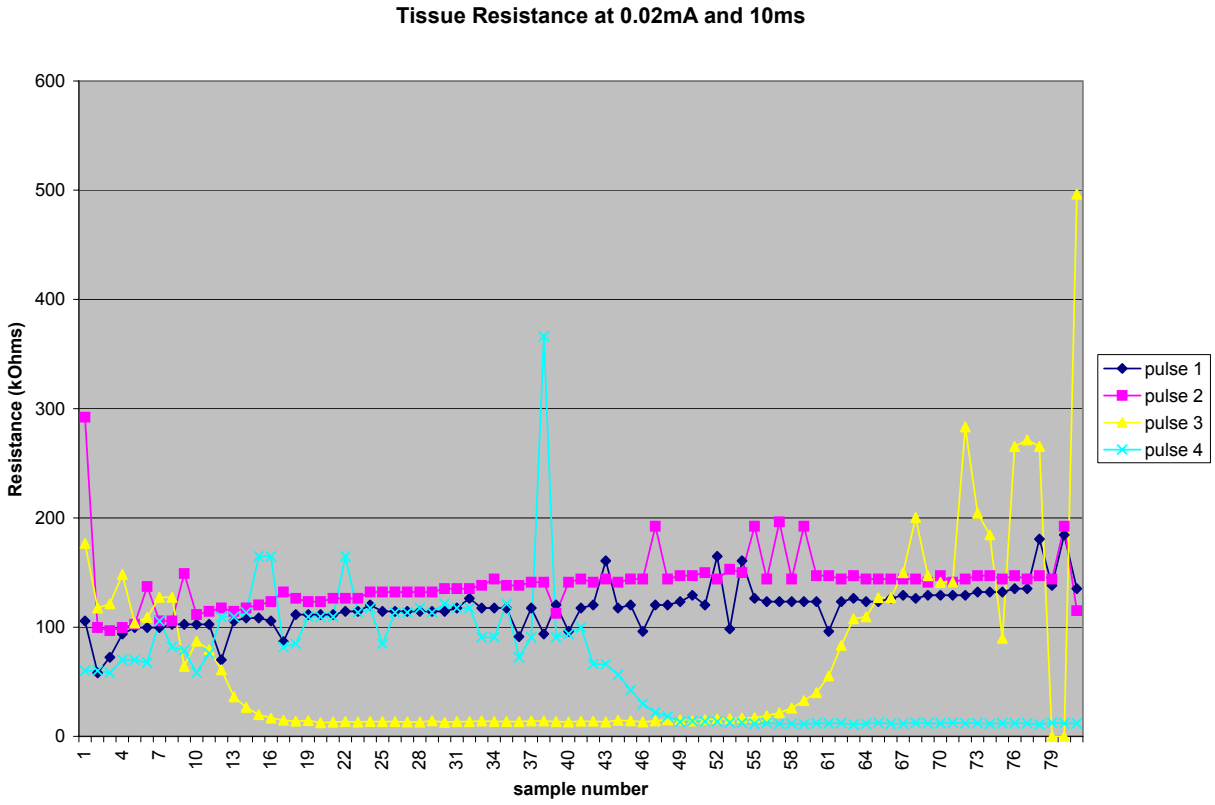
Tissue Resistance at 0.02mA and 10ms
Resistance (kOhms)
600
500
400
300
200
100
0
1
4
7
10
13
16
19
22
25
28
31
34
37
40
43
46
49
52
55
58
61
64
67
70
73
76
79
sample number
pulse 1
pulse 2
pulse 3
pulse 4

APPENDIX C

Current in the micro-amp region

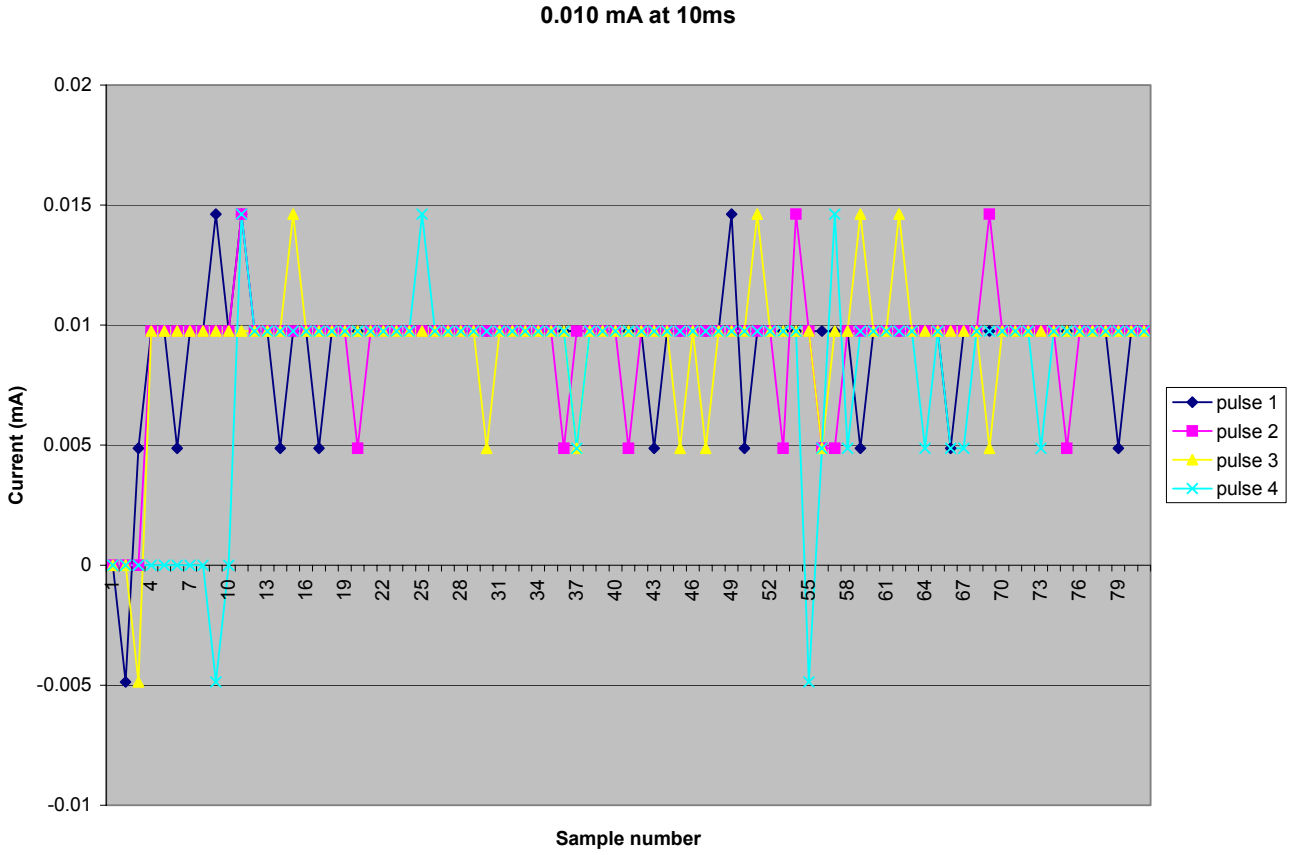

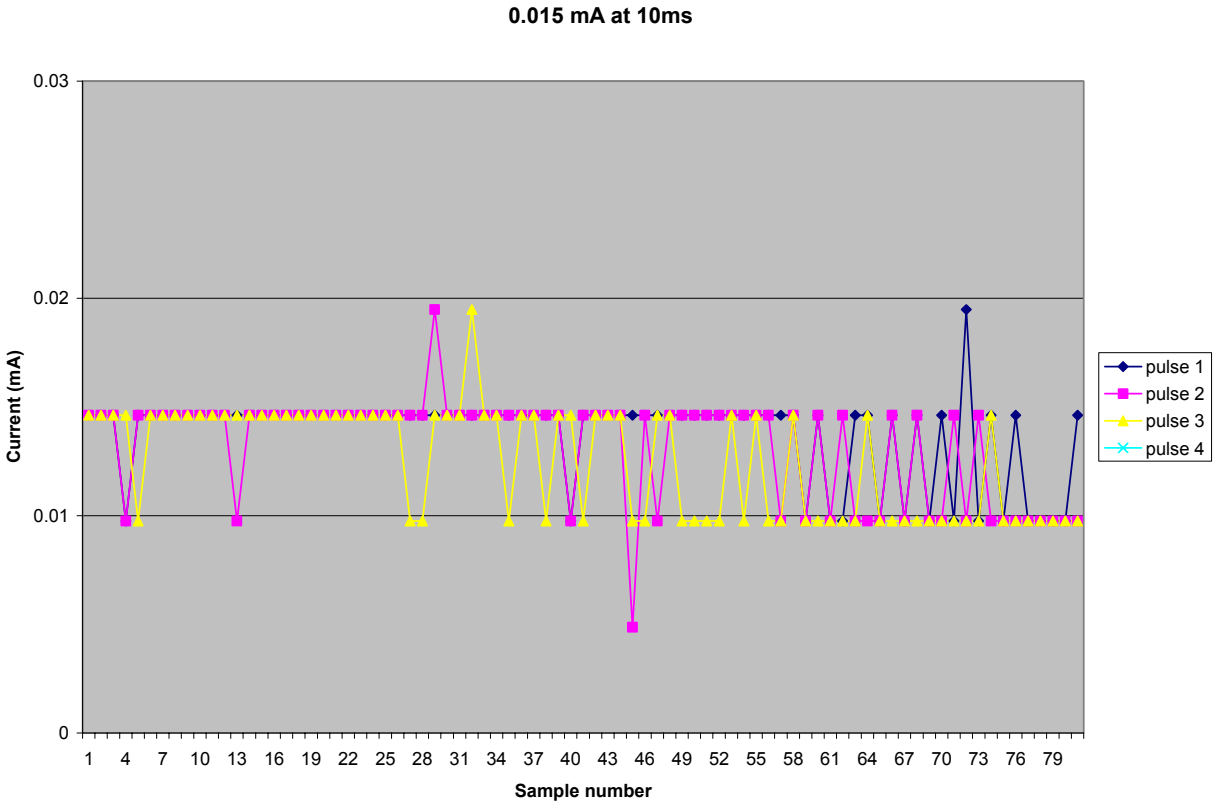
0.015 mA at 10ms
0.03
0.02
0.01
0
Current (mA)
1 4 7 10 13 16 19 22 25 28 31 34 37 40 43 46 49 52 55 58 61 64 67 70 73 76 79
Sample number
pulse 1
pulse 2
pulse 3
pulse 4

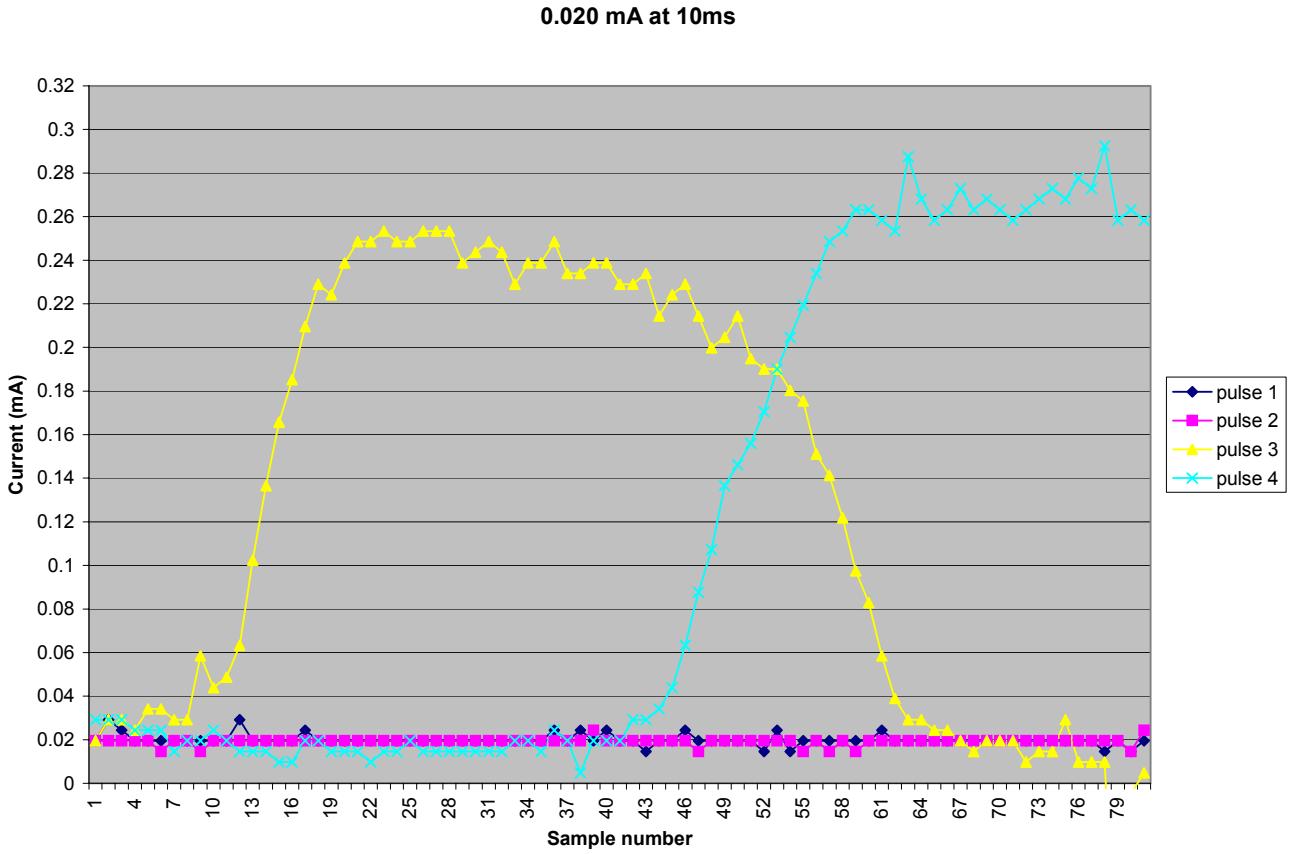
0.020 mA at 10ms
Current (mA)
0.32
0.3
0.28
0.26
0.24
0.22
0.2
0.18
0.16
0.14
0.12
0.1
0.08
0.06
0.04
0.02
0
1
4
7
10
13
16
19
22
25
28
31
34
37
40
43
46
49
52
55
58
61
64
67
70
73
76
79
Sample number
pulse 1
pulse 2
pulse 3
pulse 4

BIBLIOGRAPHY

BIBLIOGRAPHY

1. http://www.acnr.co.uk/pdfs/volume2issue3/v2i3anatomy.pdf

2. www.bellspalsy.ws/nerve.htm

3. "Reanimation of the paretic eyelid using gold weight implantation: A New Approach and Prospective Evaluation". Gilbard Steven M and Daspit C Phillip, Ophthalmic Plastic and Reconstructive Surgery, Vol. 7, p. 93-103 (1991).

4. "Facial disfigurement and psychiatric sequelae", Nordlicht S., NY State J Med, Vol. 79, p. 1383-1384 (1979).

5. "Multi-channel orbicularis oculi stimulation to restore eye-blink function in facial paralysis", Somia NN, Zonnevijlle ED, Stremel RW, Maldonado C, Gossman MD, and Barker JH, Microsurgery, Vol. 21, p. 264-270 (2001).

6. "Prospective evaluation of eyelid function with gold weight implant and lower eyelid shortening for facial paralysis", Chepeha DB, Yoo J, Birt C, Gilbert RW, Chen J., Archives of Otolaryngology-Head & Neck Surgery, Vol. 127, p. 299-303 (Mar 2001).

7. "Efficacy of gold weight implants in facial nerve palsy: quantitative alterations in blinking", Abell KM, Baker RS, Cowen DE, Porter JD., Vision Research, Vol. 38, p. 3019-3023 (1998).

8. "Surgical Management of Bell's Palsy", Gantz BJ, Rubinstein JT, Gidley P, Woodworth GG., Laryngoscope, Vol. 109, p. 1177-1188 (1999).

9. "Hypoglossal-facial nerve anastomists: its significance for modern facial palsy", Stennert E., Clinical Plastic Surgery, Vol. 6, p. 471-481 (1979).

10. "Restoration of function in long standing facial paralysis", Tucker HM., Otolaryngology Clinic North America, Vol. 15, p. 69-76 (1982).

11. "Restoration of Facial Nerve Function: An Approach for the Twenty-First Century", A. Lee Dellon, M.D., Neurosurgery Quarterly, Vol. 2, p. 199-222 (1992).

12. "Blink reflex recovery in facial weakness-An electrophysiologic study of adaptive changes", Syed NA, Delgado A, Sandbrink F, Schulman AE, Hallett M and Floeter MK., Neurology, Vol. 52, p. 834-838 (Mar 1999).

13. "The effectiveness of neuromuscular facial retraining combined with electromyography in facial paralysis rehabilitation", Cronin GW and Steenerson RL., Otolaryngology-Head and Neck Surgery, Vol. 128, p. 534-538 (2003).

14. "Bion system for distributed neural prosthetic interfaces", Loeb, G.E., Peck, Raymond A, Moore, William H. and Hood, Kevin, Medical Engineering & Physics, Vol. 79, p. 9-18 (Jan 2001).

15. "Useful Applications and Limits of Battery Powered Implants in Functional Electrical Stimulations", Lnnmuller, H, Bijak M, Mayr, Rafolt D, Sauermann S and Thomas H., Artificial Organs, Vol. 21, p. 210-212 (1997).

16. "An implantable device for stimulation of denervated muscles in rats", Dennis Robert G, Dow Douglas E, Faulkner John A., Medical Engineering & Physics, Vol. 25, p. 239-253 (2003).

17. Campbell, Neil A., Reece, Jane B., Mitchell, Lawrence G., Biology (Fifth Edition; New York: Addison Wesley Longman, Inc., 1999), pp. 968.

18. Campbell, Neil A., Reece, Jane B., Mitchell, Lawrence G., Op. Cit., p. 1016.

19. Campbell, Neil A., Reece, Jane B., Mitchell, Lawrence G., Op. Cit., p. 1016.

20. Campbell, Neil A., Reece, Jane B., Mitchell, Lawrence G., Op. Cit., p. 1017.

21. http://www.bris.ac.uk/Depts/Physiology/ugteach/ugindex/m1_index/nm_tut4/page1.htm

22. Correspondence with Dr. John Johnson and Dr. David Wood, University of Pittsburgh.

23. http://www.bio.warwick.ac.uk/andrewM/Jo%20Selwood%20site/other_rhythms.htm